UWB ANTENNA DESIGN FOR UNDERWATER COMMUNICATIONS

Aleix Garcia Miquel

25 May, 2009

Science may set limits to knowledge,
but should not set limits to imagination
Bertrand Russell

Acknowledgements

After all this year, a lot of people have contributed in some way to this thesis. I would like to show gratitude to all of them.

Firstly, I would like to thank my supervisor, Zoubir Irahhauten, for giving me the opportunity to work on this project, and for the enthusiasm, inspiration, time and effort that he has put to help me on the thesis.

I also thank my tutor, Geert Leus, and all the members of CAS. It is also a pleasure to give thanks to some members of the department of telecommunications, specially to Bill, who has helped me a lot in the complex field of the antenna design.

I would also like to thank some people of the 17th floor, particularly Antoon for helping me with all the technical troubles that I have had in the beginning, and other students that work hard in the laboratory for their good suggestions.

I also wish to thank my new friends who I met during my stay in Delft, particularly to Juanma, Caitlin, Jaime, Victor and Ana who have contributed to make possible this thesis with their kindly help. These friends and the others will be in my heart forever because of the incredible amount of unforgettable moments that we have shared.

It is also a pleasure to give thanks to my old friends from the university of Barcelona, Saul, Pau, Adri, Jordi G, Jordi S, Marc, Ruth, Vivi, Ana and many others. They have helped me to be here now, in the end of the degree.

Finally, I want to thank my parents and my sister for guiding me through the darkness and the uncertainty, for giving me unlimited love and support, things that have led me to fly higher every day.

Contents

List of Figures

List of Tables

Chapter 1

Introduction

1.1 Summary

Ultra-Wide Band (UWB) is a promising technology for many wireless applications due to its large bandwidth, good ratio of transmission data and low power cost. So far all UWB devices are designed to work in air environments. However, in this thesis UWB is introduced to operate in liquid environments (e.g. water). It can be useful for establishing communication between underwater sensors, using electromagnetic signals in distances of few meters. In such applications the antenna becomes an important element regarding the propagation aspects of the electromagnetic waves in liquid. Therefore, the main goal of this thesis is to design an UWB antenna suitable for that purpose. In order to achieve that goal, three new UWB antennas have been designed and presented, analyzing the behavior of some typical antenna parameters, such as the return loss, the radiation pattern and the directivity. Setting the dimensions of the proposed antennas to improve these parameters, it has been found a design candidate with good characteristics for our application. The size of these antennas has also been studied because of its important effect on the frequency behavior. Moreover, the parameters such as conductivity and permittivity of water have been taken into account in our antenna analysis.

1.2 Motivation for the design of an underwater UWB Antenna

A suitable antenna is needed for the Smart moving Process Environment Actuators and Sensor (Smart PEAS) project developed by the department of Circuits and Systems (CAS), Delft University of Technology, Delft, The Netherlands. The function of this Smart PEAS is to integrate it into an UWB wireless network to achieve local control and local measurement in process equipment to improve the quality of products. The main idea here is to float sensor-equipped small microelectronic devices inside certain process equipment. Such sensors apply UWB technology for transmitting large amounts of data

with very low power over relative short distances. The proper hydrodynamic design of sensors with respect to size, density, robustness and fluid compatibility enables the spatial and temporal monitoring of process variables all over the vessel. The actuation function may as well be integrated into these devices, enabling the dynamic control of different process variables.

Another motivation for the design of an underwater UWB antenna is the limited work in that kind of antennas. There are a lot of designs for UWB antennas, but most of them are done for air communications. It is needed an UWB technology to obtain a good resolution for the positioning of the devices. Furthermore, there are few studies of electromagnetic waves in water, but they have been done with narrow band antennas, such as dipoles or loops isolated with plastics. Hence the design of this antenna is a new challenge with a lot of possible solutions. In addition, the specifications for our application do not allow us to make a device bigger than 5cm of radius. This restriction in size means an extra difficulty for finding a correct antenna, mainly with a good behavior in low frequencies.

On the other hand, the propagation of electromagnetic waves in water is very different than in the air, because of its high dielectric constant. Actually, the attenuation is much higher in water, causing a limitation on the transmission distance. However, the main problem caused by it is the variation of the impedance of the antenna. This change implies a completely variation in the return loss of the antenna when it is placed in water, increasing the difficulty of the challenge.

1.3 Objectives of the thesis

The main goal of this work is to design an UWB antenna for underwater communications and its applications. One of these applications is the Smart-PEAS project, explained above. This antenna will be integrated into these sensors in order to allow the communication between them when they are placed in liquid. Our antenna has to meet some characteristics required for this project:

- The antenna has to work between 100MHz and 1GHz because an UWB behaviour is needed.
- It is also requested a transmission in frequencies as low as possible, because there the attenuation is less than in high frequencies.
- The antenna has to be omnidirectional because it will be placed in a device which will be moving.
- The size of the antenna has to be small (e.g. $r \leq 5cm$).

In addition, after finding a good design for the application, the antenna will be studied and analyzed in order to understand its behavior in different conditions. These studies will be carried out varying the parameters of the antenna, and also some characteristics of the propagation medium, such as the conductivity and the permittivity.

The goal is to find out what are the environmental conditions under which the antenna can work properly.

1.4 Organization of the thesis

This report is divided into eight chapters.

Chapter 2 provides an overview of Ultra-Wide Band (UWB) characteristics, properties of underwater propagation and classes of suitable antennas for our application. The chapter explain the fundamental antenna parameters and antenna requirements.

In chapter 3 two different softwares (Feko and Cst Microwave Studio 5) are compared to find the the most suitable for underwater applications.

Chapter 4 is dealing with the analysis of the antenna and the variations in the medium. First, some basic antennas are analyzed to find the most suitable shapes. Then, three new antennas are proposed, studying their parameters in order to achieve the antenna requirements. After that, the transmission loss between two antennas placed in water is analyzed. Finally, an analysis of the medium properties variations is presented.

In chapter 5 some conclusions and recommendations for future work are presented.

Chapter 2

Background

2.1 UWB Technology

As defined by the Federal Communications Commission (FCC), UWB technology is to transmit and receive information over a large bandwidth [9]. UWB implementations modulate an extremely short duration impulse that has a very sharp rise and fall time, thus resulting in a waveform that occupies several GHz of bandwidth (Fig. 2.1 and Fig. 2.2).

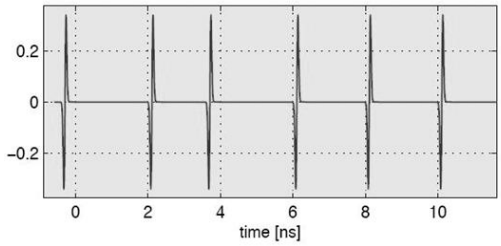

Figure 2.1: UWB transmission with pulses

These are the two conditions of UWB technology:

$$B_W \geq 500\text{MHz} \tag{2.1}$$

or

$$\frac{B_W}{f_c} \geq 0.2 \tag{2.2}$$

where f_c is the central frequency and B_W is the bandwidth.

UWB can operate between 3.1 and 10.6 GHz at limited transmission powers for indoor communications, as defined in FCC [9]. However, for our purpose, the system will work between 100 MHz and 1 GHz because the propagation will be in liquid and it won't interfere in other technologies that use this range of frequencies in air. Generally,

imaging and radar implementations of UWB transmit between 1 and 100 megapulses per second, while communications systems have between 1 and 2 gigapulses per second [1] (Fig. 2.1).

UWB was originally developed for military communications and radar. However, thanks to the good features offered, the commercial applications are increasing and UWB systems received more and more attention in the latest years.

In our application, it is needed an UWB behavior because a good resolution time is requested (and it is inversely proportional of the bandwidth). The receiver recognize the multipaths according to the resolution, and for the correct positioning of the devices this is very important.

2.1.1 UWB Advantages

Among others, we can identify the following advantages [14]:

- Possibility of high data rates.
- High resolution localization, due to the very short pulse duration.
- Channel fading resistant, due to the large number of resolvable multipath components.
- Carrier-less signal propagation.
- Overlay with existing frequency allocation, due to the low power spectral density (Fig. 2.2).
- Multiple-access capabilities, due to the wide bandwidth of transmission.
- Propagation through solid materials, due to the presence of energy at different frequencies.
- Possibility of coverting communications, with low probability of interception, due to the low power spectral density.
- Simplicity in implementation, low cost of devices.

2.1.2 UWB Applications

A combination of the UWB advantages allows some interesting applications [14]:

- High Resolution Radar. It is one of the first UWB applications, because of the fine positioning characteristics of narrow pulses. They can offer a very high resolution radar.

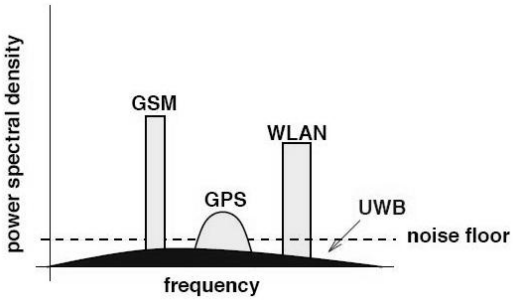

Figure 2.2: UWB and other technologies

- Wireless Personal Area Networks (WPAN). UWB is an ideal technology to replace the wires of the personal computers and their peripherals, without interfering with your local wireless network.
- Wireless Body Area Network (WBAN). It consists on a set of autonomous wireless sensors with ultra-low-power requirements spread over the human body or even implanted inside the body.
- Sensor Networks. Networks with sensors placed inside an area or volume. Low-cost and long-life battery-operated devices are very important requirements for this application.
- Location aware communications. The good performance of UWB devices in multi-path channels can provide accurate geolocation capability for indoor and obscured environments where GPS does not work.
- Military communications. The probability to detect or intercept UWB pulses are very low. Thus, the covert military communications are ideal for that purpose.
- Imaging systems, like ocean imaging, medical diagnostic and surveillance devices. UWB reflections of the target exhibit not only changes in amplitude and time shift, but also changes in the pulse shape.
- Vehicular radar systems. Detection of the position and movement of objects near the vehicle are more accurate thanks to UWB devices.
- Emergency Situations. UWB signals can penetrate obstacles because of the wide frequency spectrum. This property is very useful to detect and rescue survivors under rubble in disaster situations.

2.2 Signal Propagation in Water

The most used waves to establish underwater wireless communications are the acoustic waves. However, acoustic communications are limited by two factors: low speed of

sound underwater and time-varying multipath propagation. Together, these factors result in a communication channel of poor quality and high latency. Optical systems are another alternative to take into account, but they usually fail because of suspended matter of the liquid medium.

There are many applications that need a fast communication between two or more devices within short distances. In this case, it is better to use electromagnetic waves because their properties are more suitable. To study the positioning of the sensors, the system has to work fast because the position of sensors could change very fast as well, and with the acoustic waves we could make a lot of mistakes causing slow propagation. In fact, Maxwell's equations give us the speed of electromagnetic waves in a medium. While for acoustic waves this speed of propagation is over 1440 m/s in water, for electromagnetic waves this propagation works over 33.5×10^6 m/s (2.3), becoming more than 23×10^3 times faster.

$$v = \frac{1}{\sqrt{\varepsilon\mu}} \tag{2.3}$$

where v is the speed of electromagnetic propagation in a medium, μ is the permeability (in water is $1.256 \times 10^{-6} N/A^2$) and ε is the permittivity (in water is $707 \times 10^{-12} F/m$). Note that the electromagnetic propagation in water is only about 9 times slower than in free space. This has important advantages for command latency and networking protocols in underwater communications, where information has to be exchanged between different sensors [2].

In addition, Doppler shift is inversely proportional to propagation velocity, so it is much smaller for electromagnetic signals:

$$\triangle f = -\frac{f v_{rel}}{c} \tag{2.4}$$

where f is the transmitted frequency, v_{rel} is the velocity of the transmitter relative to the receiver in meters per second (negative when moving towards one another, positive when moving away) and c is the speed of wave (e.g. 33.5×10^6 m/s for electromagnetic waves traveling in water).

2.2.1 Conductivity

The conductivity of water is dependent on its concentration of dissolved salts and other chemical species which tend to ionize in the solution. The purer the water is, the lower the conductivity will be (the higher the resistivity will be). The conductivity is also dependant on the temperature, as Table 2.1 shows [14].

These are the typical values of water conductivity [17]:

- Ultra pure water: 5.5×10^{-6} S/m
- Distilled water: 0.001 S/m
- Drinking water: $0.005 - 0.05$ S/m

Table 2.1: Electrical conductivity (S/m) of sea water

Temperature ($C°$)	Salinity (g/Kg)		
	20	30	40
0	1.745	2.523	3.285
5	2.015	2.909	3.778
10	2.300	3.313	4.297
15	2.595	3.735	4.837
20	2.901	4.171	5.397
25	3.217	4.621	5.974

- Sea water: $4 - 5.3$ S/m
- Great Salt Lake, USA: 15.8 S/m

2.2.2 Permittivity

With a relative dielectric permittivity (ε_r) of 81 at 20°C of temperature and at 1GHz of frequency [15], water has among the highest permittivity of any material and this has a significant impact in the behavior of the electromagnetic waves propagation. However, this value experiences variations with the frequency and the temperature. Figure 2.3 shows the dielectric constant in dependance of the frequency and the temperature. The arrows show the effect of increasing temperature or increasing water activity. [18]. The wavelength range 0.01 - 100cm is equivalent to 3THz - 0.3GHz respectively. The purpose of this section is to study the permittivity in a range between 10MHz and 1GHz. As it can be noticed, for that range the dielectric constant does not vary with the frequency. Hence it can be assumed a constat ε_{water} of 81 when the temperature is about 20°C and the frequency is less than 1GHz.

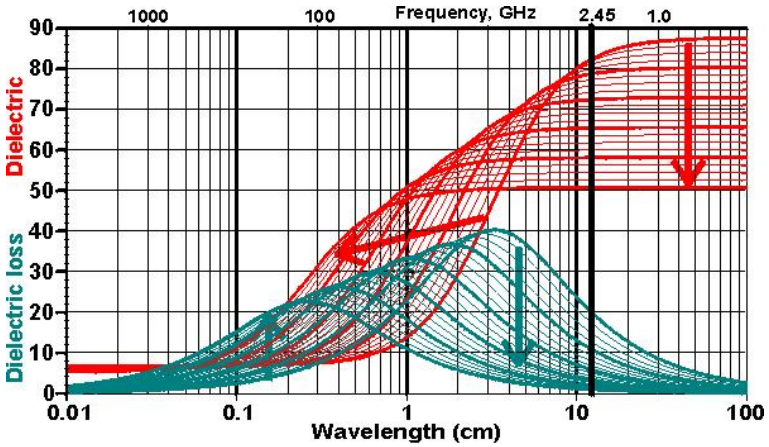

Figure 2.3: Dielectric permittivity and dielectric loss of water between 0°C and 100°C

The permittivity in water is dependant on this relative permittivity (ε_r), the permittivity of the vacuum ($\varepsilon_o = 8.85 \times 10^{-12}$) and the conductivity ($\sigma$), as the equation (2.5) shows:

$$\varepsilon_{water} = \varepsilon_o \varepsilon_r - j\frac{\sigma}{\omega} \tag{2.5}$$

If the imaginary component appeared due to the conductivity is not taken into account, and we take a relative permittivity of 81, the permittivity in water is 707×10^{-12} F/m.

2.2.3 Propagation

As far as we know, the electromagnetic propagation through water is very different from propagation through air because water has high permittivity and electrical conductivity.

Maxwells equations are very important to predict the propagation of electromagnetic waves traveling into water. A linearly polarized plane electromagnetic wave propagating in the z direction may be described in terms of the electric field strength E_x and the magnetic field strength H_y with [3]:

$$E_x = E_o \exp(j\omega t - \gamma z) \tag{2.6}$$

$$H_y = H_o \exp(j\omega t - \gamma z) \tag{2.7}$$

where E_o is the original electric field and H_o is the original magnetic field. The propagation constant γ is expressed in terms of the permittivity ε, permeability μ and conductivity σ by:

$$\gamma = j\omega\sqrt{\varepsilon\mu - j\frac{\sigma\mu}{\omega}} = \alpha + j\beta \tag{2.8}$$

where α is the attenuation factor, β is the phase factor, and ω is the angular frequency ($\omega = 2\pi f$). The term $\varepsilon\mu$ arises from the displacement current and the term $\sigma\mu/\omega$ from conduction current. It is convenient to consider the solutions for the conduction band $\sigma/\omega > \varepsilon$ and the dielectric band $\sigma/\omega < \varepsilon$.

Investigations of the parameters σ and ε over the full electromagnetic frequency spectrum have been obtained in electrolytic solutions by using a wide variety of experimental techniques [3].

In the conduction band, plane wave attenuation in water is highly compared to air, and increases rapidly with frequency [4]:

$$\alpha = 0.0173\sqrt{f\sigma} \tag{2.9}$$

where α is the attenuation in dB/m, f is the frequency in Hz and σ is the conductivity in S/m.

If we have pure water (σ=0), we are in the dielectric band, where the attenuation is less than 10dB/m at frequencies lower than 1GHz.

2.2.4 Wavelength

Knowing the relationship between the wavelength λ, the speed v and frequency f as (2.10)) shows:

$$\lambda = \frac{v}{f} \tag{2.10}$$

and with (2.1) which shows the value of speed in the water, we get that the frequency under water is about 9 times lower than in free space:

$$f_{water} \approx \frac{f_{air}}{9} \tag{2.11}$$

2.2.5 Intrinsic Impedance

In addition, the intrinsic impedance, η,(2.12) changes too. For a region with slightly electrical conductivity ($\sigma > 0$, e.g. seawater), the impedance is given by (2.13), and in a region with no conductivity ($\sigma = 0$, e.g. free space), the impedance simplifies to (2.14). In pure water the equation simplifies to (2.15):

$$\eta = \frac{E}{H} \tag{2.12}$$

$$\eta = \sqrt{\frac{j\omega\mu}{\sigma + j\omega\varepsilon}} \tag{2.13}$$

$$\eta_{freespace} = \sqrt{\frac{\mu}{\varepsilon}} \approx 377\Omega \tag{2.14}$$

$$\eta_{purewater} = \sqrt{\frac{\mu_{purewater}}{\varepsilon_{purewater}}} \approx 42\Omega \tag{2.15}$$

In addition, Figure 2.4 shows the absolute value of the intrinsic impedance at four different frequencies (50MHz, 100MHz, 150MHz and 200MHz) in water with different conductivities. It is observable that the impedance decreases with the conductivity, but increases with the frequency.

It can be also observed the real part and the imaginary part in Figure 2.5.

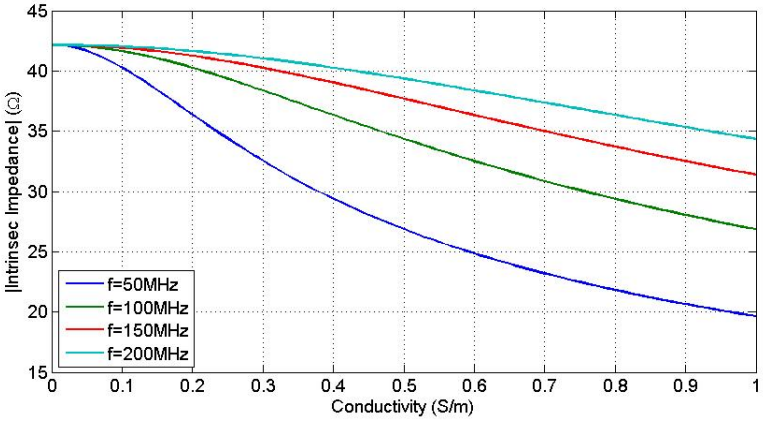

Figure 2.4: Intrinsic impedance on dependance of the conductivity of different frequencies in MHz

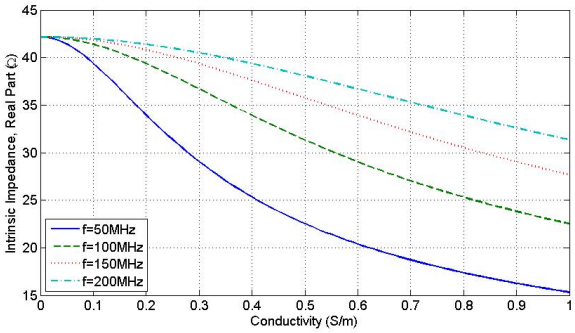

(a) Real part

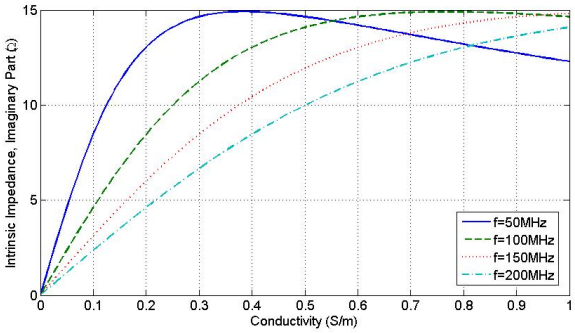

(b) Imaginary part

Figure 2.5: Real part and imaginary part of the intrinsic impedance on dependance of the conductivity of different frequencies in MHz

2.3 Basic Antenna Parameters

A background of the fundamental antenna parameters is presented in order to understand the physical behavior of the antenna and also to improve its performance. These antenna parameters are directly obtained by a professional electromagnetic solver (CST Microwave Studio 5 or FEKO)[11].

2.3.1 Return loss

In a transmission line, when an incident wave propagates along it, V^+, a fraction of the voltage amplitude is reflected, V^- due to the impedance discontinuities. The reflection coefficient, Γ, is defined as:

$$\Gamma = \frac{V^-}{V^+} = \frac{Z_L - Z_S}{Z_L + Z_S} \tag{2.16}$$

where Z_L is the impedance towards the load and Z_S is the impedance towards the source.

In our case we have a single pair of input/output terminals, referred to one port. The corresponding scattering matrix consists on a single element, the scattering parameter or reflection coefficient S_{11} [12].

$$b_1 = S_{11} \times a_1 \tag{2.17}$$

where a_1 is the incident wave in the port and b_1 is the reflected wave in the port. The return loss of an antenna (RL) is calculated by:

$$RL = -10 \log_{10} |S_{11}|^2 = -10 \log_{10} |\Gamma|^2 \tag{2.18}$$

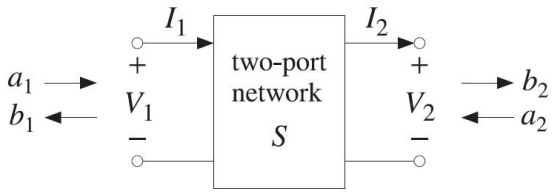

Figure 2.6: Simple circuit configuration showing the ports location

2.3.2 Radiation Pattern

The antenna radiation pattern is defined as the spatial distribution of a quantity which characterizes the electromagnetic field generated by an antenna [13]. It is possible to represent the radiation pattern of an antenna using three dimensions or two dimensions,

on both spherical and polar coordinate systems respectively. The two dimensional radiation pattern can be used to determine the relative strength of the radiation power in the far field with regard to the direction. On the spherical coordinate system two different planes are particulary interesting: the E-plane (the plane containing the electric field vector and the direction of maximum radiation) and the H-plane (the plane containing the magnetic field vector and the direction of maximum radiation)

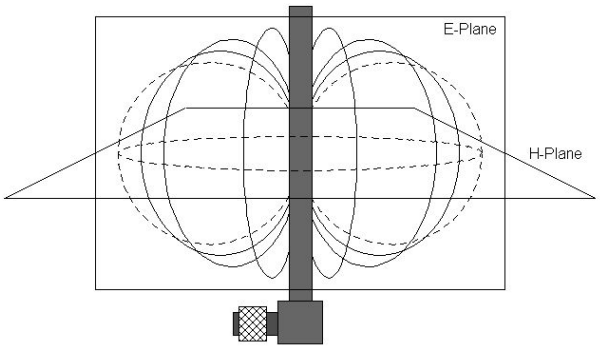

Figure 2.7: E-plane and H-plane for a dipole antenna

In this thesis we are going to study the gain. The level of this parameter is related with the power of the feeding. With the directivity, it allows to know the efficiency of the antenna.

2.3.3 Directivity

The directivity in a direction measures the power density that an antenna radiates in a specific direction, relative to the power density radiated by an ideal isotropic radiator antenna radiating the same amount of total power.

This parameter is related with the power of radiation, and it is used to know the efficiency of the antenna with the equation (2.19).

$$G = N \times D \tag{2.19}$$

where G is the gain, D is the directivity, and N is the efficiency of the antenna.

2.4 Underwater Antennas

The main goal of the project is designing an antenna for UWB underwater communications. But first we have to know which antennas are more suitable for propagation into water. Published references [5] indicate that loop antennas, long wires and dipoles have been successfully used underwater at very low frequencies. Because of the reduction of the frequency shown in the equation (2.11), their physical dimensions are lower than their equivalent in space.

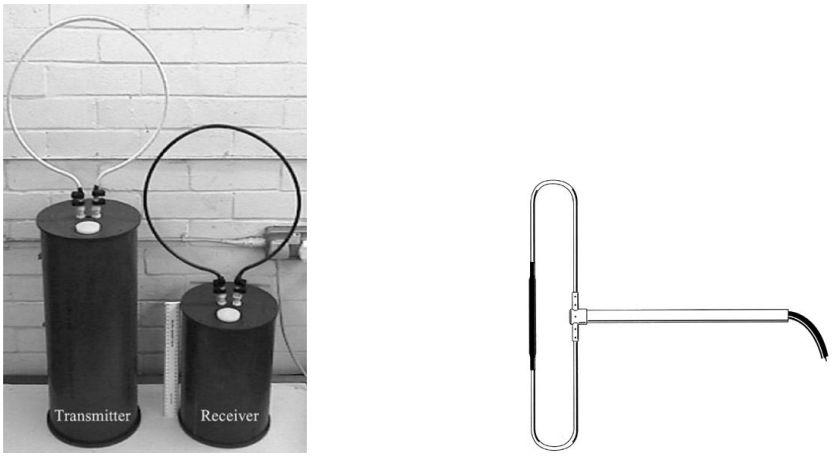

(a) Circular loops (b) Folded dipole

Figure 2.8: Different classes of underwater antennas

Historically, in the underwater communications, antenna conductors are insulated from the water to prevent leakage of direct current to the conducting medium. But this is not our goal. We are going to design a small antenna with the conductors directly touching water because of the small size required [1].

2.5 UWB Antennas

There are three different classes of UWB antennas based on different applications [8]:

DC-to-daylight: These antennas are designed to have maximum bandwidth and to use as much spectrum as possible. Typical applications are ground penetrating radars, field measurements or electromagnetic compatibility, impulse radars, and shelter communication systems.

Multi-narrowband: The design goal of multi-narrow band antennas is similarly to grab as much spectrum as possible but to only use small sub-bands at any given time. These antennas are designed as scanner or signal intelligence antenna for receiving or detecting relatively narrowband signals through certain frequencies.

Modern: These are antennas designed for use in conjunction with the approximately 3:1 bandwidth, as 3.1-10.6 GHz UWB systems authorized by the FCC (Federal Communications Commission). The bandwidth requirements for a modern UWB antenna are narrower than for DC to daylight antennas. These antennas have certain implication that distinguish them from the other more traditional classes of UWB antennas. First, instead of trying to grab maximal bandwidth, these modern UWB antennas must operate within a certain spectral mask. In this context, excessive bandwidth degrades system response and is counterproductive.

Second, unlike multi-narrowband antenna, a modern UWB antenna potentially uses much, if not all, of its bandwidth at the same time. Thus, a modern UWB antenna must be well behaved and consistent across the antennas operational band. Its properties include radiation pattern, gain, antenna matching, and requirement for low or no dispersion. A wide variety of antennas meets the demands of modern UWB system.

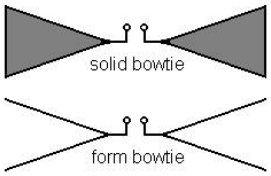

(a) Bow-tie

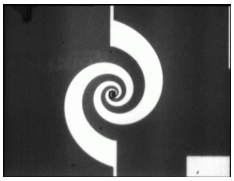

(b) Spiral

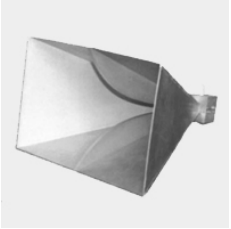

(c) Horn

Figure 2.9: Different classes of UWB antennas

Otherwise, the antennas for UWB technology can be divided into the following group based on the characteristics [8]:

Frequency independent antennas: Antennas whose mechanical dimensions are short compared to the operating wavelength are usually characterized by low radiation resistance and large reactance. This combination results in a high quality level and consequently a narrow bandwidth. The current distribution on a short conductor is ideally sinusoidal with zero current at the free end, but because the conductor is so short electrically, typically less than 30 of a sine wave, the current distribution will be approximately linear. By end loading to give a constant current distribution, the radiation resistance is increased four times, thus greatly improving the efficiency but not noticeably altering the pattern. Because the effective source of the radiated fields varies with frequency, these antennas tend to be dispersive. Examples of frequency-independent antennas include spiral, log periodic, and conical spiral antennas.

Horn antennas: A horn antenna is an electromagnetic funnel concentrating energy in a particular direction. Horn antennas tend to have high gain and relatively narrow beams. Horn antennas also tend to be large and bulkier than small-element antennas. These antennas are well suited for point-to-point links or

other applications where a narrow field of view is desired. As an example we can mention the TEM (Transverse Electromagnetic mode) horn antenna.

Reflector antennas: A reflector antenna also concentrates energy in a particular direction. Like horn antennas, reflector antennas tend to have high gain and are relatively large. Reflector antennas tend to be structurally simpler than horn antennas and are easier to be modified and adjusted by manipulating the antenna feed.

Small element antennas: These antennas tend to be small, omnidirectional antennas well suited for commercial applications. Examples of small element antennas include Lodges biconical and bow-tie antennas, diamond dipole, ellipsoidal antennas, and Thomass circular dipole.

2.6 Antenna Design Requirements

To design our specific antenna, the parameters described in Section 2.3 should be taken into account, and the final shape should satisfy different specifications such as physical size and electrical performance.

- As far as the electrical performance is concerned, the antenna should be able to transmit a pulse having a bandwidth ($|S_{11}| \leq$-10 dB) located in the range from 100 MHz to 1 GHz (wide bandwidth implies a good resolution time). A return loss level lower than -10 dB means that more than the 90% of the energy is radiated.

- The omnidirectionality of the antenna is another important requirement, because this antenna should transmit in all directions, thus the radiation pattern should be as much omnidirectional as possible.

- The size is another important factor in this project, because the final application requires a small antenna with a diameter around 5-10 cm. This restriction is the hardest specification due to the relationship between the size and the frequency. For lower frequencies as required in the specifications, the size should be bigger. Thus, the design of a small antenna becomes a challenging issue.

Chapter 3

Tools for Underwater Antenna Simulations

Usually, antenna designers use some kind of software to simulate the response of the antennas to be able to analyze the results and to determine the best shape for each application. However, these applications are normally for air, and the simulation tools of these softwares are prepared for that purpose and not for underwater applications. It has been tested two of the most used softwares (FEKO and CST Microwave Studio 5) in different conditions to determine which one is the best for underwater applications.

First, we analyze the differences between both softwares. We explain the reason because FEKO is better than CST when simulating antennas in water. Second we simulate a dipole with FEKO and with CST to be able to check the differences. Finally, we give some conclusions about the behavior of each software.

3.1 Software Characteristics

In this section we give an overview of the most interesting differences of the simulation tools between both softwares (FEKO and CST Microwave Studio 5). There are more interesting tools. However, by analyzing these characteristics, we will be able to determine which one is the best software for the applications in mediums with a high permittivity.

3.1.1 The Mesh

Both softwares are very good for simulations in air. However, the high permittivity of the water makes the simulations more difficult. Each software uses a different way to solve the simulations, and it depends basically of the mesh used to determine the antenna's area or volume of interest. Each software is more suitable depending on the application.

In the application that we study, we need simulations in water with a permittivity of 81. That means that we need a dense mesh to obtain good results. Nevertheless, if

the mesh is too dense, the software is not able to solve the simulation. The choice of the correct mesh is one of the most important and hard decisions.

In CST software, the mesh is three-dimensional. The solver takes a determinate volume of the background where the shape is placed, and analyzes all the volume with the mesh. The shape of the mesh cells is rectangular (Figure 3.1a). In order to choose an appropriate mesh in CST, we have to modify some parameters:

Lines per wavelength This value is connected to the wavelength of the highest frequency set for the simulation. It defines the minimum number of mesh lines in each coordinate direction that are used for a distance equal to this wavelength. In a way, it sets the spatial sampling rate for the signals inside of your structure. This setting has a strong influence on the quality of the results and on the calculation time. Increasing this number leads to a higher accuracy, but unfortunately also increases the total calculation time.

Refine at PEC / lossy metal edges by factor This option increases the spatial sampling at PEC (Perfect Electric Conductor)or lossy metal edges. At these edges additional density points are added that force the automatic mesh generator to increase the mesh density at those points by the given factor. This setting is very useful, because at metal edges you theoretically obtain singularities in the electromagnetic fields. This means, that the fields vary very much near such edges and have to be sampled higher than elsewhere.

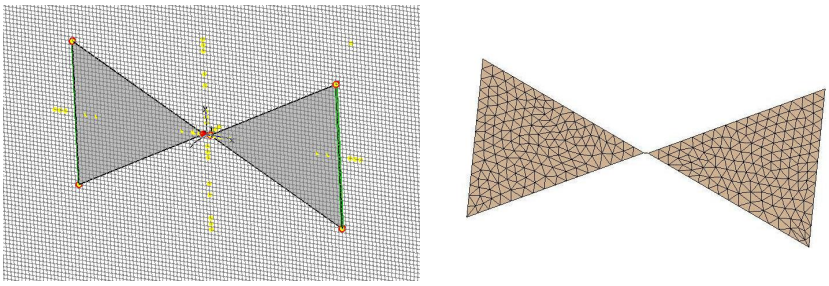

(a) CST (b) FEKO

Figure 3.1: Different meshes

Otherwise, FEKO software works in a different way. The solver only takes the surface or volume needed, but not the background. The shape of the cells is triangular (Figure 3.1b). To choose a correct mesh in FEKO, we have to determine the size of the cells. We can try a bigger size for the big faces of the shape, but we should choose a small size for other faces and for the edges, because there are more singularities in the electromagnetic fields, and they have big variations.

When working into water, a weighty mesh is needed due to the high permittivity. Thus, the software more suitable is FEKO, because the number of cells needed is lower (that means less execution time in simulations), and also the triangular shape gives us

a better precision. Moreover, FEKO shows warnings and errors more accurately than in CST.

3.1.2 The Background Properties

In CST Microwave studio 5 we do not have the opportunity to change more parameters than the relative permittivity (ε_r). Otherwise, in FEKO we can change more parameters, such as the conductivity (σ) or the dielectric loss factor ($\tan\delta$) , which have a direct effect in the permittivity (ε) (eq. 3.1 and 3.2).

$$\varepsilon = \varepsilon_o\varepsilon_r - j\frac{\sigma}{\omega} \tag{3.1}$$

$$\varepsilon = \varepsilon_o\varepsilon_r(1 - j\tan\delta) \tag{3.2}$$

Both parameters depend on the kind of water used. However, we are not going to analyze these parameters now.

In the next chapter an analysis of the dipole's behavior is shown in order to check if there are more differences between FEKO and CST.

3.2 Analysis of a Dipole Antenna

If we analyze a basic halfwave dipole (wavelength of 4m) in air and in water, we should find a similarity between theoretical and empirical results. We test the empirical results with FEKO and CST, with the same conditions (Table 3.1) in each case. However, the mesh depends of the software used.

Table 3.1: Range of frequencies to simulate

Case	Range	Samples
$\varepsilon_r = 1$	0-500MHz	200
$\varepsilon_r = 25$	0-100MHz	200
$\varepsilon_r = 81$	0-50MHz	200

We are going to take into account the frequencies and the magnitudes of the first and second minimums and the distance between them. The distance between these two minimums is important if we want to know if the frequency of the minimums is coherent in each case.

We have already seen the theoretical results in Section 2.2, specifically in equations (2.3, 2.10 and 2.11).

To get the dipole's work frequency, we use:

$$f = \frac{c}{\lambda} = \frac{\frac{c_o}{\sqrt{\varepsilon_r}}}{\lambda} \tag{3.3}$$

where c_o is the speed of the vacuum ($3 \times 10^8 m/s$).

3.2.1 Case 1: $\varepsilon_r = 1$ (Air)

First of all, we analyze the behavior of the return loss of the dipole in air (Figure 3.2).

In FEKO, we obtain that the antenna is matched around 71.2MHz, while the theoretical result is 75MHz (equation 3.3). The next frequency with a minimum return loss is 221.7MHz. Hence, the distance between both frequencies is 165MHz.

In CST, the antenna is matched at 73.7MHz, and the next minimum is in 221.7MHz. The distance is 148MHz.

Both graphics are very similar in low frequencies, but the third minimum is not exactly the same. We can also see that the level of the first minimum is better (lower) in FEKO than in CST.

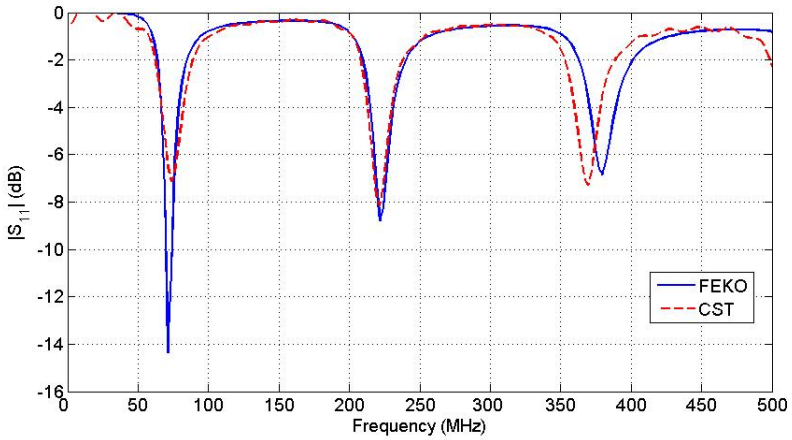

Figure 3.2: S_{11} of a dipole in air

3.2.2 Case 2: $\varepsilon_r = 25$

If we apply the equation 3.3 in this case, we obtain that the work frequency is 15MHz.

Figure 3.3 shows us that both simulations are very similar. The first minimum is at 15.4MHz, and the second one is at 45.7MHz. The difference is 30.3MHz. However, the first frequency matched is located in the third minimum, at 77MHz. Hence we see that the impedance has changed.

Due to the theory, we know the frequencies should be the same in this case, but divided by $\sqrt{\varepsilon_r}$ when we change the background. Thus, taking the difference between the two minimums in air, the new differences should be 29.6MHz in CST ($148/\sqrt{25}$) and 30.1MHz ($150.5/\sqrt{25}$). These values are close to the empirical result of 30.3MHz found in the simulations.

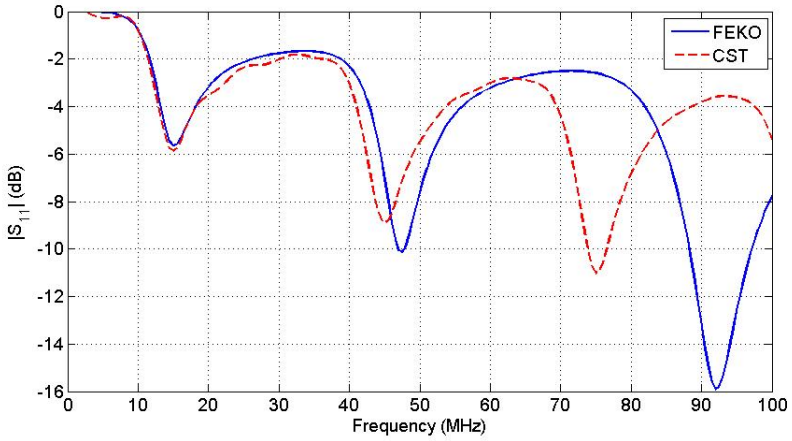

Figure 3.3: S_{11} of a dipole in a background with a relative permittivity of 25

3.2.3 Case 3: $\varepsilon_r = 81$ (Water)

Finally, we put the dipole in water (ε_r of 81). From (3.3) we know that the work frequency is 8.3MHz.

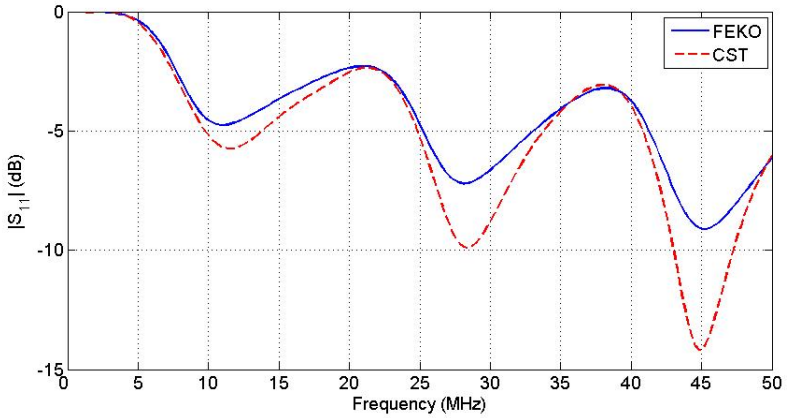

Figure 3.4: S_{11} of a dipole in water

Figure 3.4 shows us the simulation. In FEKO the first minimum is at 11.1MHz, while the second one is at 28MHz. The separation between them is 16.9MHz, close to the 16.7MHz theoretically obtained ($150.5/\sqrt{81}$).

In the CST simulation, the first minimum is at 11.6MHz, and the second one at 28.3MHz. The difference is exactly 16.7MHz, as the theory indicates.

The frequencies are close to the theory in both softwares, but the level of the $|S_{11}|$ is very different. If we try to improve the mesh, we obtain the same results in FEKO, and in CST the level approaching to the FEKO's one.

3.3 Conclusions

Table 3.2 compares the results between FEKO and CST.

Table 3.2: Results of the simulations (in MHz)

Case	Theory	CST	FEKO
$\varepsilon_r = 1$	75	73.7	71.2
$\varepsilon_r = 25$	15	15.4	15.4
$\varepsilon_r = 81$	8.3	11.6	11.1

It can be concluded that the results of the simulations are similar to the results of the equations. However, when we increase the permittivity, the lower frequencies are not matched. That means that the impedance in water changes, and we have to solve it by improving the parameters of the shape.

Furthermore, it is interesting to know which software takes more time to run the simulations, because when the permittivity is very high, the time of the simulations increases. The Table 3.3 shows the time of the simulations.

Table 3.3: Times of the simulations

Case	CST	FEKO
$\varepsilon_r = 1$	1min	7sec
$\varepsilon_r = 25$	9min	10sec
$\varepsilon_r = 81$	35min	1min

In this table we can observe that CST delayed faster than FEKO in high permittivities. These results are manageable times, but when the range of frequencies increases, the time increases too. Specially in CST software, the simulations can be delayed for several hours. For example, if the frequency range is from 0 to 1GHz, the simulation of the dipole in water takes more than 2 hours in CST. On the other hand, in FEKO software the same simulation just takes few minutes.

To get correct results, the mesh has to be improved in each case. When the permittivity increases, the density of the mesh has to be increased too. In CST this operation implies a long simulation time.

In addition, as we can see in the Figures 3.2 and 3.3, the simulations in CST have curls in some low frequencies, but not in FEKO.

And also we have to remember Section 3.1.2, where it was told that in FEKO it is possible to change more background parameters than CST, allowing a complete study of the antenna behavior.

Hence, it can be finally concluded that FEKO is more suitable than CST to simulate antennas for underwater applications.

Chapter 4

Antenna Analysis

This chapter is dealing with the analysis of the requested antenna. First, we test some candidate shapes that we think that could be suitable for the application. For example, the circular loop, which is usually used in underwater communications (Section 2.4), and some typical antennas used in UWB systems (Section 2.5). After that, we combine the most suitable shapes to achieve an antenna that meets the requirements. Then, a parametric study of the dimensions is performed to find the best design.

Finally, once the antenna has been selected, we analyze the behavior of the shape when changing the properties of the medium.

4.1 Basic Shapes

In this section we study simple shapes in air and we will compare the obtained results when the antenna is put in water. First, we consider the circular loop because it shown a good behavior in water (see Section 2.4). After that, we will study some typical UWB antennas, such as the circular dipole, the diamond and the bow-tie antenna. We want to test the possibility of using them in water because their response in air could be similar to that in water, but in a bandwidth 9 times lower, and with a different return loss level (because the impedance depends of the environment, as we have seen in Section 2.3.1). Finally, we will compare all the results to choose the best shape for our application. In FEKO software we can obtain the return loss, the phase and the radiation pattern.

To study these shapes, we choose sizes close to radius of 5cm, because it is the maximum size permitted by the requirements. In air, the range of frequencies analyzed is from 10MHz to 9GHz, with 200 samples . Otherwise, because in water the frequencies are 9 times lower, the studied range is from 10MHz to 1GHz, also with 200 samples. The reason for this choice is that the frequencies in water are 9 times lower than in air, and also we want to study the behavior in low frequencies.

The feeding in both cases do not have to touch water because it is needed a electrical device to feed the antenna. In the air simulations this is not a problem, but in the

water simulations we have to isolate the feeding. In these cases, the isolation is done by putting the feeding inside a small region with free space.

4.1.1 Circular Loop

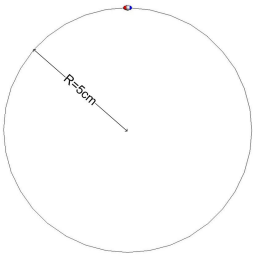

Figure 4.1: Dimensions of circular loop antenna

To study the behavior of the circular loop we use a circular wire with a radius of 5cm (Figure 4.1). We analyze the differences between the response in air and in water to check the viability of this shape for our purpose.

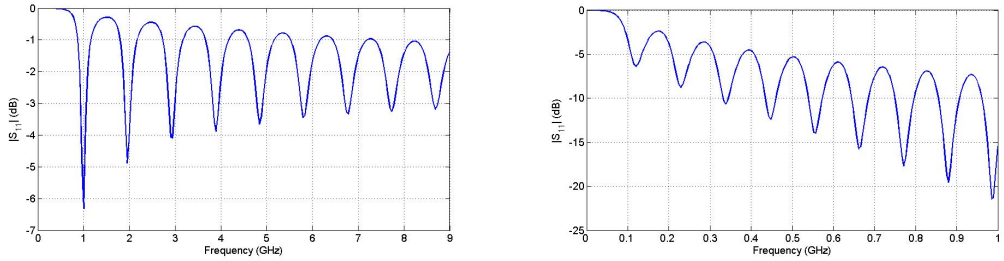

(a) in air (b) in water

Figure 4.2: S_{11} of circular loop

As we can observe in Figure 4.2, the return loss in air at 1GHz is above the level of -10dB. The dimensions of the antenna are chosen just to study these two responses, both in air and in water. In water we can see that in frequencies close to 1GHz the level of $|S_{11}|$ is better.

Thus, it has been concluded that the circular loop presents a better behavior in water environment than in air. This shape could be a good start for the design of the antenna that we are looking for the application.

4.1.2 Circular Dipole

It has been shown that a circular loop could be a good antenna, but it has to be an UWB antenna, and that is the reason why some UWB antennas in water have been studied.

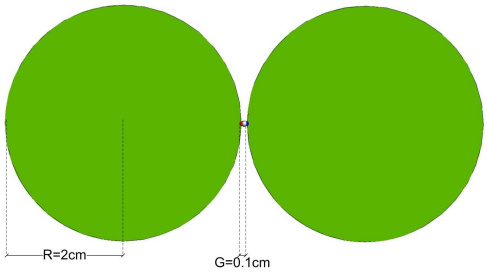

Figure 4.3: Dimensions of circular dipole antenna

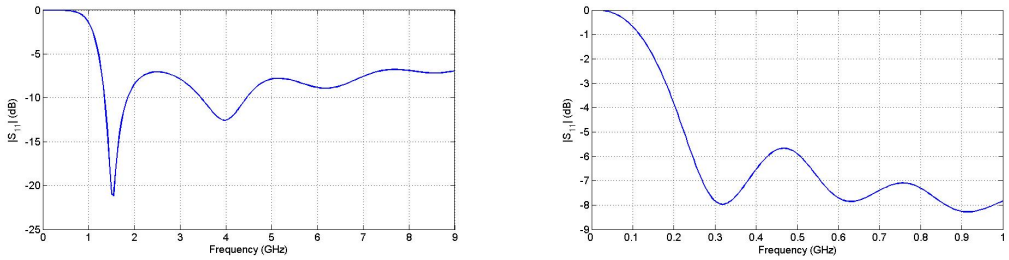

(a) in air (b) in water

Figure 4.4: S_{11} of a circular dipole

The response of the circular dipole of Figure 4.3 is presented in Figure 4.4. It can be observed that in air is not exactly UWB. That could be because the purpose of this section is to check the differences within the two behaviors and not to design the typical antenna for a commercial UWB application. In water, the return loss at low frequencies does not meet our requirements. Hence, the circular dipole is not a good initial shape for the design of the final antenna.

4.1.3 Bow-tie (Standard shape)

The bow-tie is also a typical UWB antenna, used for a lot of applications, and with a great variety of forms. Figure 4.5 shows a basic shape of the bow-tie antenna used for the simulation. As it can be observed in Figure 4.6, the behavior in air is not completely UWB, maybe because of that purpose we should modify some parameters of this antenna, like the opening. However, the level of return loss in water starts to be less than -10dB at a low frequency (270MHz), and the bandwidth is almost UWB. Therefore, it can be concluded that bow-tie could be an interesting shape for the design of the new antenna.

Nevertheless, it is very important to get lower frequencies below the level of -10dB. To do that, we should enlarge the shape, but it is not possible because of the requirements.

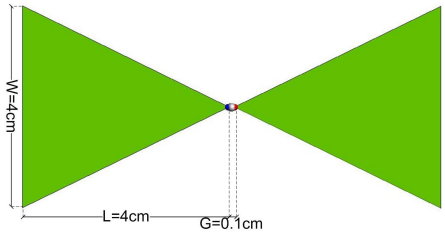

Figure 4.5: Dimensions of bowtie antenna

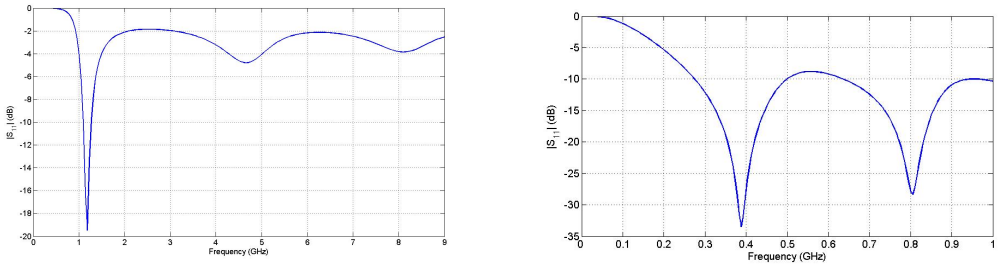

(a) in air (b) in water

Figure 4.6: S_{11} of a bow-tie antenna

4.1.4 Bow-tie (Diamond shape)

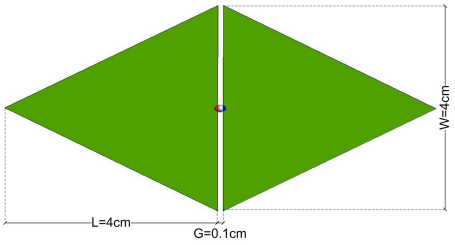

Figure 4.7: Dimensions of diamond antenna used in FEKO simulation

Finally, another kind of UWB antenna is shown (Figure 4.7). Although not totally UWB because of the size, this antenna is more suitable in air than bow-tie antenna, as we can see in Figure 4.8. However, water changes its behavior, and the return loss level starts to be the expected at relatively high frequencies (800MHz).

In that case it can be concluded that diamond antenna is worst than standard

bow-tie antenna for underwater environments.

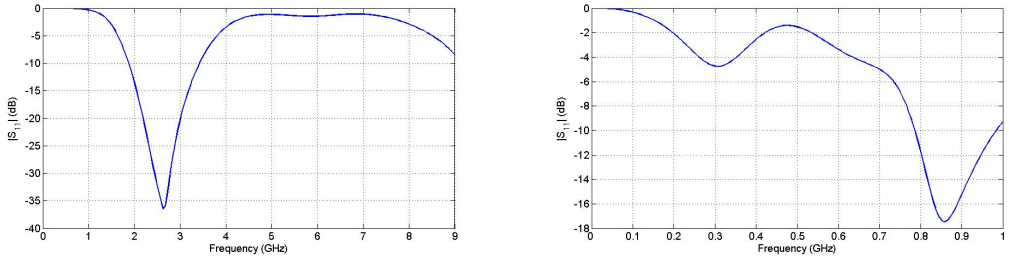

(a) in air (b) in water

Figure 4.8: S_{11} of a diamond antenna

4.2 Folded Bow-tie Antenna: First shape

After the analysis of some typical UWB antennas, it has been concluded that circular loop and bow-tie antennas are the most suitable for the underwater application. The combination of both shapes may arise into a new antenna.

The simulations are done completely in FEKO, using an accurate mesh to ensure reliable results. The most important characteristics taken into account are:

- The return loss must be less than -10 dB from a low frequency around 100MHz.
- An UWB behavior is needed.
- The antenna has to be omnidirectional.
- The size of the shape cannot measure more than 5cm of radius.

As far as we know, the application uses small devices to work. Hence the antenna size has to be as smaller as possible. This restriction is very important to determine the low frequency from which the return loss level becomes minor than -10dB. Figure 4.9 shows the dimensions of the first candidate:

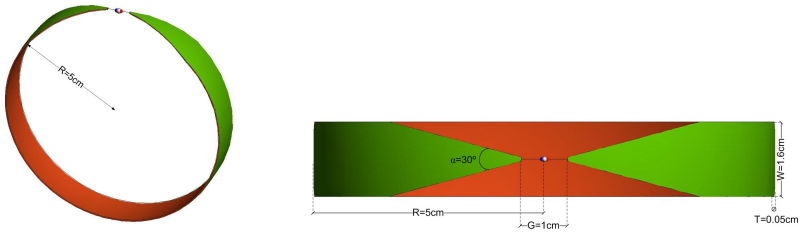

(a) Perspective view (b) Top wiew

Figure 4.9: First candidate: original antenna dimensions

The gap feeding is 1cm because it is not isolated yet. In the parametric analysis of the next sections we will isolate the feeding and we will check the best measure.

The results of the FEKO's simulation indicates:

1. The return loss is less than -10dB from 150MHz (Figure 4.10).
2. The behavior is UWB because the bandwidth is greater than 500MHz (Figure 4.10).

4.2.1 Parametric study

The parametric study of the first candidate is presented, for which the parameters to be analyzed are:

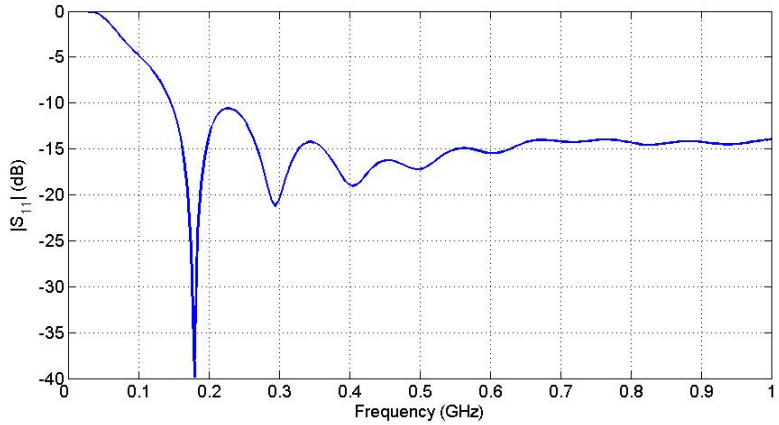

Figure 4.10: S_{11} of original first candidate

- Angle (α)
- Width (W)
- Thickness (T)
- Feeding (G)
- Size (R)

The original parameters are shown in Figure 4.9. These original values have been taken because they are similar of the typical bow-tie and loop parameters. Variations of each parameter are compared to the original one. Finally, the most suitable antenna will be found.

Angle

First, we check if the original angle ($\alpha = 30°$) has the best response.

As it can be seen in Figure 4.11a, there is another opening angle better than the original. In fact, an angle of $\alpha = 20°$ implicates a return loss level lower than with an angle of $\alpha = 30°$. Notice that this angle is the minimum possible for this shape, thus is not possible to choose an angle less than $\alpha = 20°$ because the width would have to be changed. In a new section some angles will be studied changing the width.

Width

In this section the width of the shape is studied. The original one has a width of 1.6cm.

However, as it can be seen in Figure 4.11b, a width of 2.4cm is better.

The results of the parametric study of the angle and the width lead us to think that it is possible to improve the return loss changing the width an the angle at the same

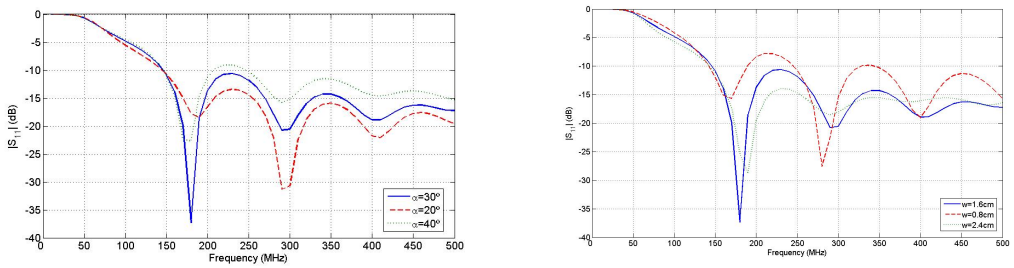

(a) Angle (b) Width

Figure 4.11: $|S_{11}|$ of the first candidate changing some parameter

time. The best combination occurs when the cut from the feeding finishes in the half of the antenna.

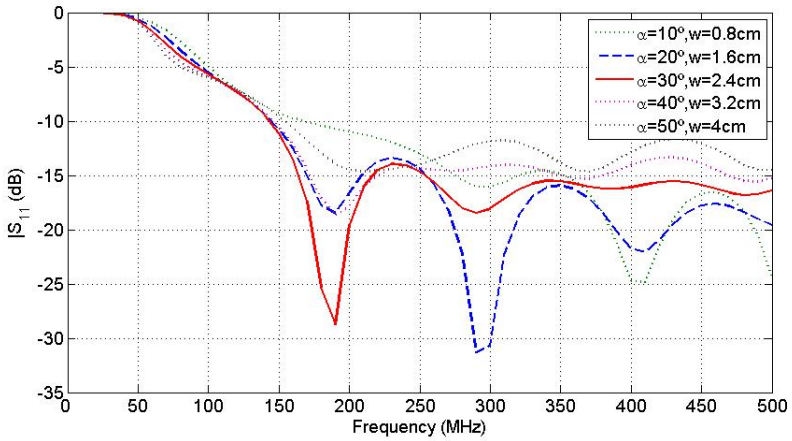

Figure 4.12: $|S_{11}|$ with different widths and angles

Hence, these five combinations are tested:

- Width=0.8cm. Angle=5°
- Width=1.6cm. Angle=10°
- Width=2.4cm. Angle=15°
- Width=3.2cm. Angle=20°
- Width=4cm. Angle=25°

Figure 4.12 shows the combinations within the width and the opening angle. It is possible to observe that there are two options better than the others: the width of 1.6cm and the width of 2.4cm. To discern the best option, we take the antenna with

a width of 2.4cm and the angle of $\alpha = 30°$ because it starts to have lower frequencies below -10dB before than the other candidate.

Thickness

We study the thickness of the shape. The original antenna has a thickness of 0.05cm. We test 0.01cm and 0.1cm.

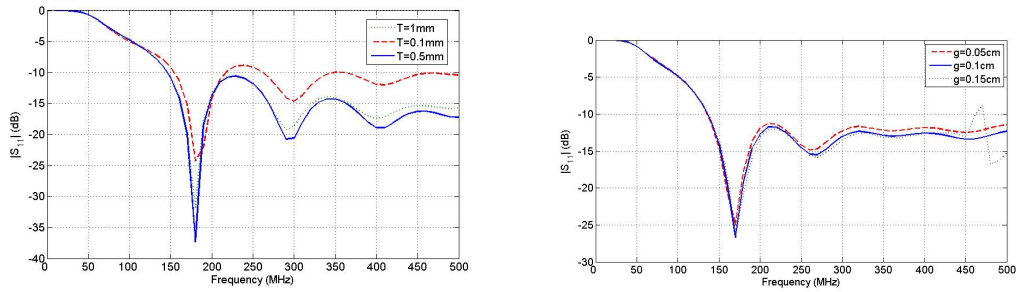

(a) Thickness

(b) Gap feeding

Figure 4.13: $|S_{11}|$ of the antenna changing some parameter

Figure 4.13a shows us that the best thickness is 0.05cm because the return loss has a lower level.

Feeding

As far as we know, the application for which the antenna is needed requires an isolated feeding. A region of free space has been placed in the gap of the shape to achieve this purpose. The original gap feeding was 1cm, but when we put this region of free space, the dimension becomes 9 or 10 times smaller, and $|S_{11}|$ has a similar behavior.

Figure 4.13b shows that the best distance is 1mm for an isolated feeding.

Up to this point, the original air region had the same dimensions as the gap between the two parts of the antenna. However, the dimensions of this region (Figure 4.14a) can be variable because for the construction of this antenna a greater isolated region is needed.

Four sizes have been tested, as Table 4.1 shows.

Table 4.1: Tested dimensions (in cm) of the air region to isolate the feeding

Case	Width (FW)	Depth (FD)	Height (FH)
Original one	0.04	0.1	0.05
First case	0.2	0.4	0.2
Second case	0.4	0.8	0.3
Third case	0.8	1.6	0.4

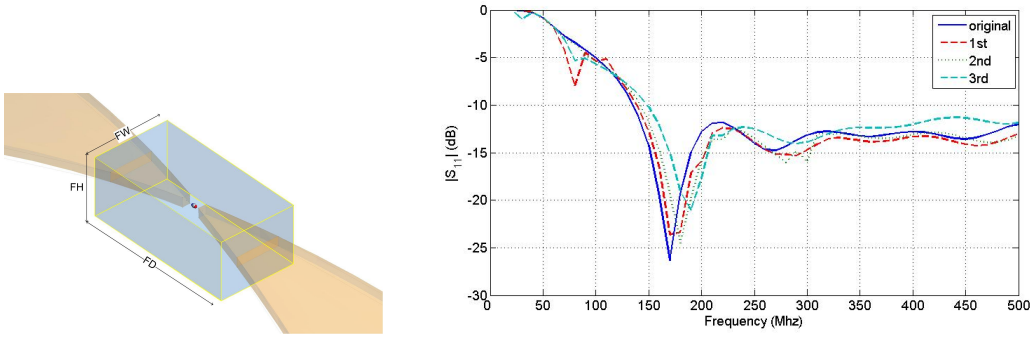

(a) Studied parameters of the isolated region

(b) S_{11} of the first shape with different air regions

Figure 4.14: Isolated region of the first candidate

From Figure 4.14b it can be observed that the levels of the return loss do not have a significant change in high frequencies, because in all the range the level is below the boundary of -10dB. Nevertheless, in low frequencies next to the beginning of the bandwidth, a trend is appreciable. The bigger is the region, the later decreases $|S_{11}|$ under -10dB.

This event has a theoretical explanation. As it is exposed in the other old reports of background theory, it is known that frequencies in water are over 9 times smaller than in the air. Thus, if the air region is bigger, there is more part of the antenna touching air and no water. In that way, it seems logical to see that the biggest region candidate (the third one) starts to be less than -10dB at 150MHz, while the smallest one (the original one) starts at 135MHz.

To decide the final shape, it is needed to know how preferential is the size of this isolated region face up to the behavior of the return loss in low frequencies.

We are going to take the third candidate (FW=0.8cm, FD=1.6cm, FH=0.4cm).

Size

The requirements impose a size with a radius minor than 5cm. We have checked that it is not possible to obtain a frequency lower than 150MHz with this size. However, we study the variation of $|S_{11}|$ with the size to know which is the size that allows us to have -10dB from 100MHz. We have checked a scaling factor of 0.5 (radius of 2.5cm) and 1.5 (radius of 7.5cm).

In fact, as Figure 4.15 shows, a radius of 7.5cm (scaling factor of 1.5) gives the desired behavior, but with a size too big for the requirements.

Final dimensions

If we combine all the best parameters found, the result is a folded bow-tie antenna with these new dimensions.

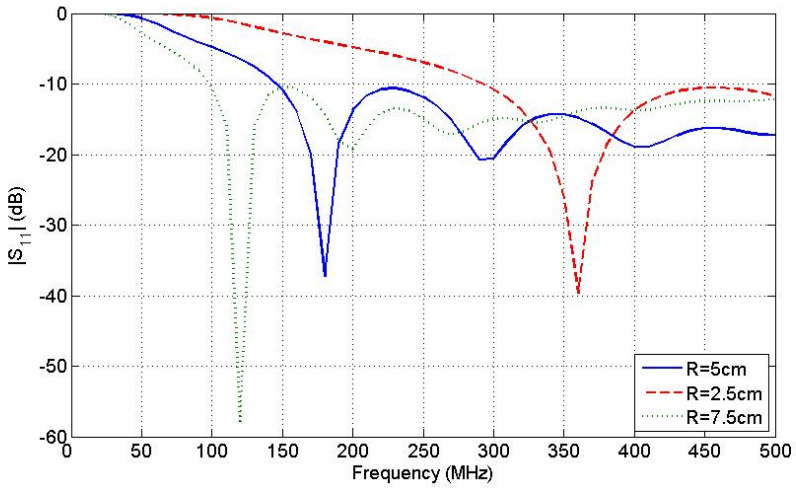

Figure 4.15: $|S_{11}|$ of the antenna with different size

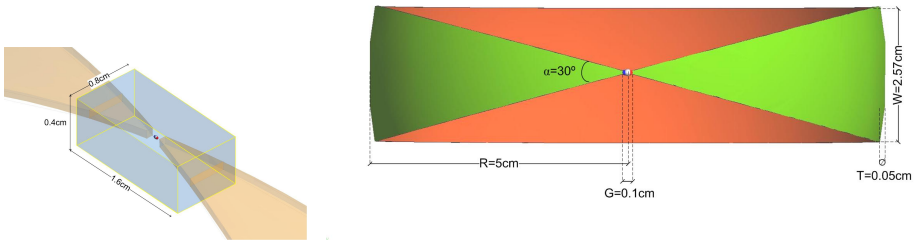

(a) feeding region (b) top view

Figure 4.16: Dimensions of the final antenna

Thus, the dimensions of the new antenna are shown in Figure 4.16, the return loss in Figure 4.17, and the radiation pattern in Figure 4.18.

The results of the FEKO's simulation indicates:

1. The return loss is less than -10dB from 135MHz (Figure 4.17) face up to the 150MHz of the original shape.

2. The behavior is UWB because the bandwidth is greater than 500MHz, it is from 135MHz to 1800MHz. Thus, the bandwidth is 1665MHz (Figure 4.17). Specifically, the relative bandwidth is more than 0.2, the minimum required to become UWB:

$$\frac{BW}{f_c} = \frac{1665}{((1665)/2) + 135} = 1.73 > 0.2 \tag{4.1}$$

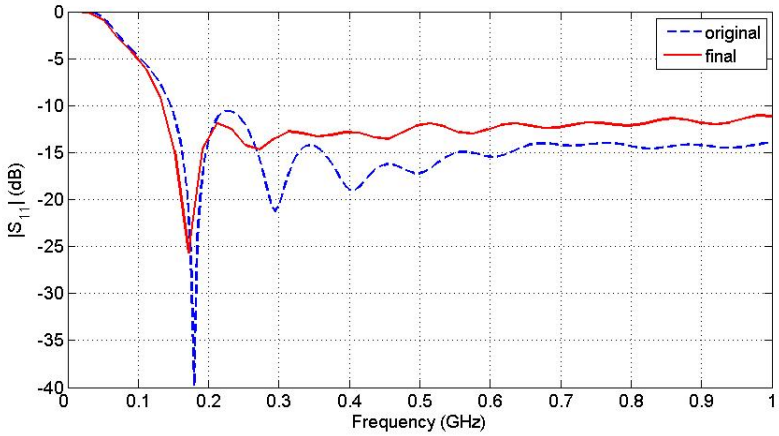

Figure 4.17: S_{11} of the new antenna and the old one

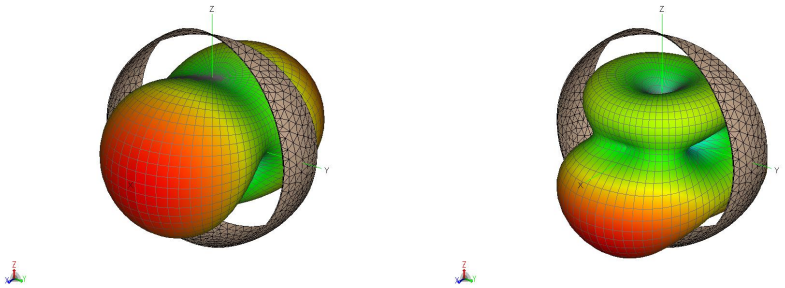

(a) 151MHz

(b) 292MHz

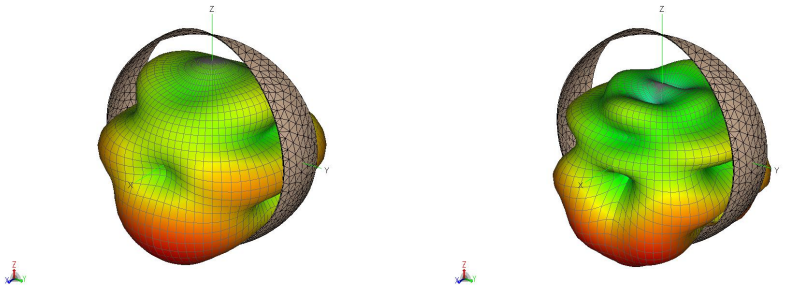

(c) 454MHz

(d) 596MHz

Figure 4.18: Radiation pattern of the first candidate without internal isolation

3. The final antenna has a better return loss in low frequencies than the original one, but in high frequencies the opposite happens. However, the low frequencies are more important than the higher ones in the water propagation because the attenuation is lower. Thus, it is more important to have a good return loss level

at low frequencies.

4. The radiation pattern is almost omnidirectional (Figure 4.18). It is not totally omnidirectional because when the length of the ring is greater than a half wave dipole, they appear some new nulls and some new lobes in the pattern. Figure 4.19 helps to understand this kind of behavior: in the first case, the wavelength is much more greater than the length of the dipole. In the second case, the antenna is a halfwave dipole (from this length they will appear a new secondary lobe). In the third case, the dipole has the same length as the wavelength, and the radiation pattern has two main lobes. Finally, in the fourth case, there are more secondary lobes. Thus, the higher the frequency is, more lobes the radiation pattern has.

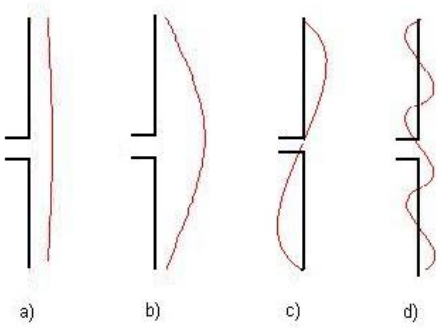

Figure 4.19: Dipoles with different lengths related to the wavelength

4.2.2 Final shape with internal isolation

The antenna needs a battery and a circuit to work, but they cannot be touching water. Thus we have to isolate the center of the antenna with a sphere. In this section we will study the behavior of the antenna when an air ball or an air-teflon ball (teflon has an ε_r of 2.1) is placed inside the antenna, as Figure 4.20 shows.

The boundary of the air ball in the first case is touching the antenna. On the other hand, the air-teflon ball is almost the same, but with a half centimeter of teflon recovering the air. This is important because air and water have to be, obviously, separate.

Furthermore, the air region of the feeding has to be improved. Otherwise, in the air-teflon ball case, we have added one millimeter of teflon to separate air and water (Figure 4.21b).

The behavior of the antenna is presented in the next sections.

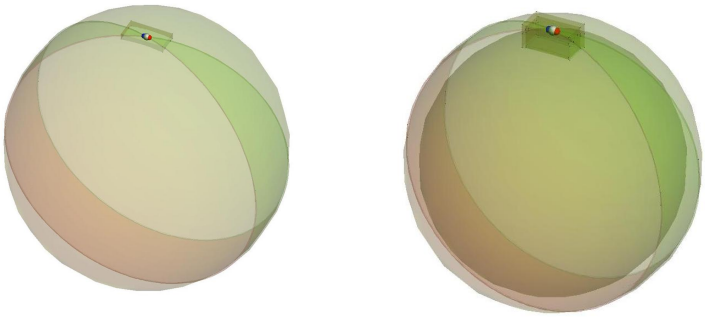

(a) air ball (b) air-teflon ball

Figure 4.20: First candidate with internal isolation

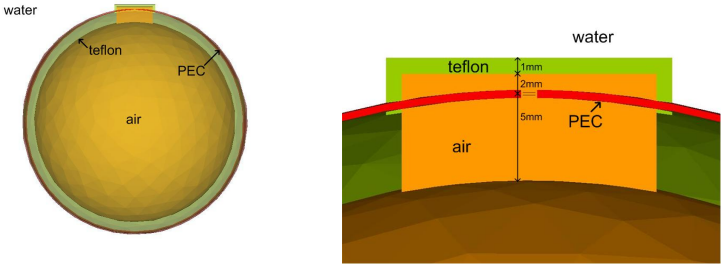

(a) front view (b) zoom of the feeding zone

Figure 4.21: Materials and dimensions of first candidate with an air-teflon isolation

Return loss

As far as we know, the return loss level is one of the most important parameters to take into account. Specially a good matching in low frequencies is needed, where the propagation in water is better. Figure 4.22 shows the $|S_{11}|$ results of the three models proposed of the first antenna candidate: the antenna without internal isolation, with an air ball, and with an air-teflon ball.

First, we check that in low frequencies the internal isolation allows the transmission in lower frequencies (almost 100MHz), while without this isolation the return loss is lower than -10dB since 135MHz. However, if we take a look at the high frequencies, the behavior is the opposite: the internal isolation reduces the transmission in high frequencies (660MHz in case of air-teflon ball and 800Mz in case of air ball), while in the model without any isolation ball the transmission is possible in frequencies higher than 1GHz.

As Table 4.2 shows, the three models are UWB because the bandwidth is greater than 500MHz, but there is a lot of difference in the behavior of high frequencies between the isolated antenna and the antenna without isolation. However, as we explained before, in water the most important range of frequencies is the range of low frequencies

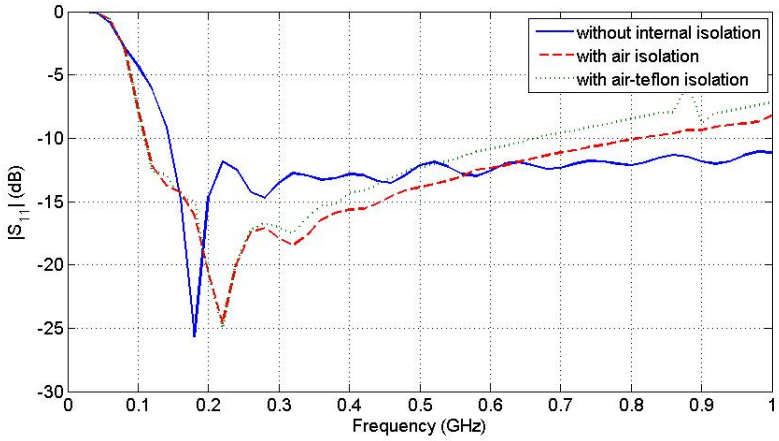

Figure 4.22: S_{11} of the first candidate: with and without internal isolation

Table 4.2: Important values of S_{11} of the fist candidate: with and without internal isolation

Case	f_1	f_2	BW
Without internal isolation	135MHz	1.6GHz	1465MHz
With an air ball of isolation	110MHz	800MHz	690MHz
With an air-teflon ball of isolation	110MHz	660MHz	550MHz

because the propagation there is better than in high frequencies. That means that the models with the internal isolation work better for our purpose.

Radiation Pattern

Another very important question is the radiation pattern of the antenna. It will be interesting to get as most omnidirectional pattern as possible in all directions to allow the communication between two of these antennas in random positions. Thus the behavior of the radiation in every direction is checked, and this is the reason because the 3D radiation pattern firstly is checked.

As Figures 4.23,4.24 and 4.25 show, the behavior of the radiation pattern in each case is totally different:

- At low frequencies (over to 200MHz) the radiation pattern of the three models is almost the same. The pattern is omnidirectional in the XY plane. In the model without internal isolation it is possible to observe that it appears a secondary lobe on the top of the shape. In the others patterns that does not occur because the permittivity in the center of the antenna is different, and it changes the wavelength of the radiate waves. And as it has been explained before, the lobes appears when the length of the ring of the antenna is greater than a half-wave

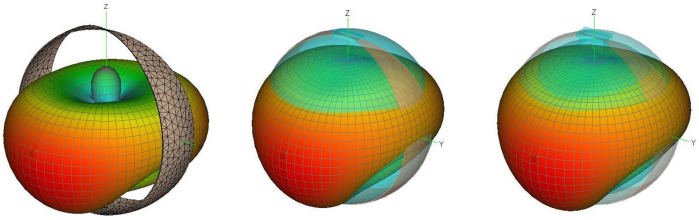

(a) without internal isolation (b) with air isolation (c) with air-teflon isolation

Figure 4.23: 3D radiation pattern at 191MHz

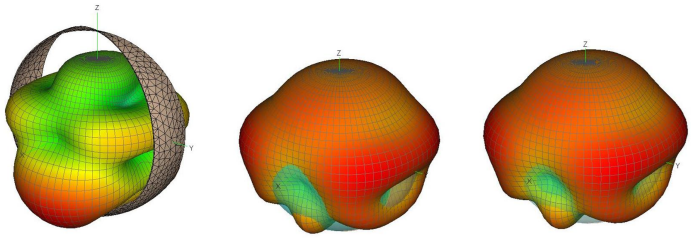

(a) without internal isolation (b) with air isolation (c) with air-teflon isolation

Figure 4.24: 3D radiation pattern at 393MHz

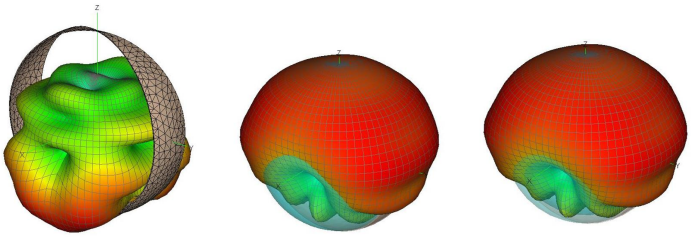

(a) without internal isolation (b) with air isolation (c) with air-teflon isolation

Figure 4.25: 3D radiation pattern at 596MHz

dipole.

- At higher frequencies (over to 400MHz and 600MHz) the pattern is very different between the cases. In the first model, the intensity of the signal is transmitted mostly in the bottom of the shape, while in the cases with isolation the intensity is above all in the top. Furthermore, when the antenna has internal isolation, the pattern is more omnidirectional. Notice also that there are more lobes in all the patterns, due to the smaller length of the wavelengths.

However, when the antenna is in the liquid medium, it will be floating, moving

and rotating all the time. Thus, it can be concluded that the three models of the first candidate are almost omnidirectional.

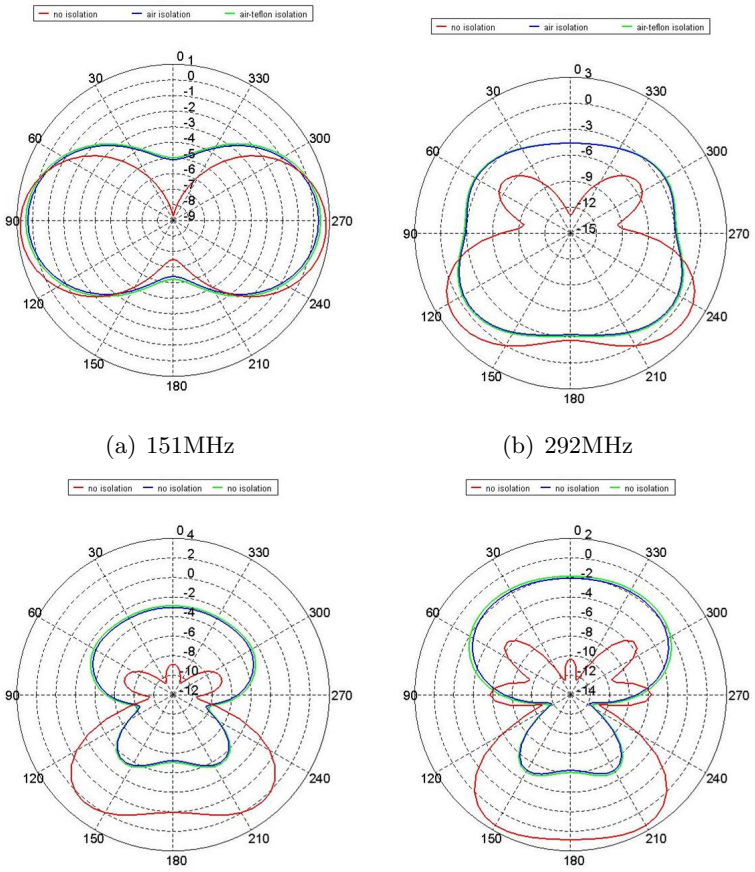

(a) 151MHz (b) 292MHz

(c) 454MHz (d) 596MHz

Figure 4.26: Radiation pattern of the gain (in dB) in 2D (XZ plane) at different frequencies

Also the radiation pattern in two dimensions can be analyzed, specifically in the middle of the antenna, in the XZ plane (Figure 4.26).

In this case the values of the gain in dB can be seen, in some frequencies in the range of interest. Almost in all the frequencies this value is between -10dB and 0dB. These levels related with the levels of directivity of the next section indicates that the efficiency of the antenna is not very good because the difference between the gain and the directivity is about 3dB.

Directivity

To understand better the far field intensity of the most significantly directions, a study of the directivity in dependance of the frequency in the top (Z direction), the middle

(X direction and Y direction) , and the bottom of the antenna (-Z direction); can be done, as Figure 4.28 shows.

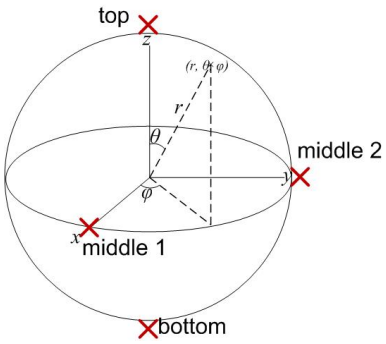

Figure 4.27: Spherical coordinates and points of interest

Analyzing the results for each case, it is possible to conclude that:

- The antenna without internal isolation radiates better in the middle 1 (X direction) at low frequencies (from 135MHz to 250MHz), while at frequencies from 250MHz it radiates with more intensity in the bottom. It can also be appreciated that in the top (Z direction) and in the middle 2 (Y direction) of the shape the radiation is not very appropriate because it oscillates too much.

- In the cases of air and an air-teflon isolation, the radiation is higher in the middle 1 at frequencies between 100MHz and 350MHz, but from 350MHz the major directivity is in the top of the shape and in the middle 2.

It is also interesting to realize that almost all the levels of the directivity remain between -10dB and 5dB. If the radiation pattern was totally omnidirectional, the directivity would be 0dB in all the directions (like a perfect sphere). Otherwise, if the radiation pattern was directional, the directivity would be more than 0dB in some directions and less than 0dB in the rest of the pattern. Hence it can be concluded that the directivity of this antenna is different in each case and in each direction. Nevertheless, because of the continuous movement of the device where the antenna will be placed, the behavior is quite correct.

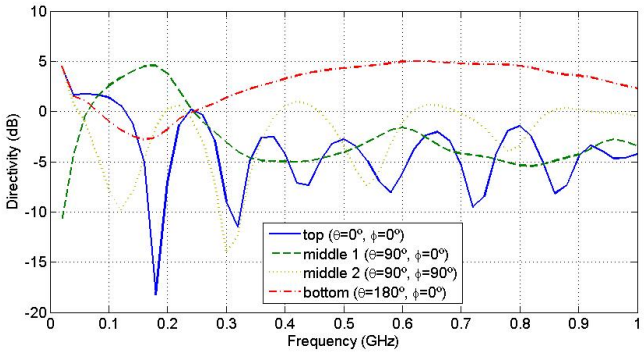

(a) antenna without internal isolation

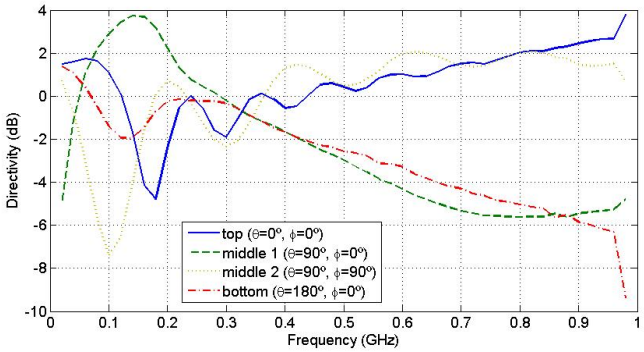

(b) antenna with air isolation

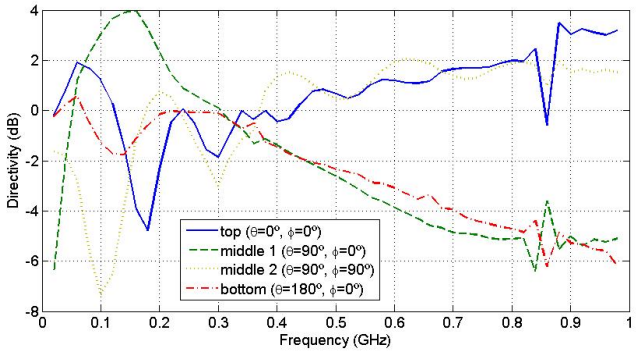

(c) antenna with air-teflon isolation

Figure 4.28: Directivity in dependance of the frequency

4.3 Folded Bow-tie Antenna: Second shape

The second candidate is also a folded bow-tie loop antenna. However, now the angle α is not chosen on the top, it is chosen on the side, as Figure 4.29 shows. This is the main difference from the first candidate.

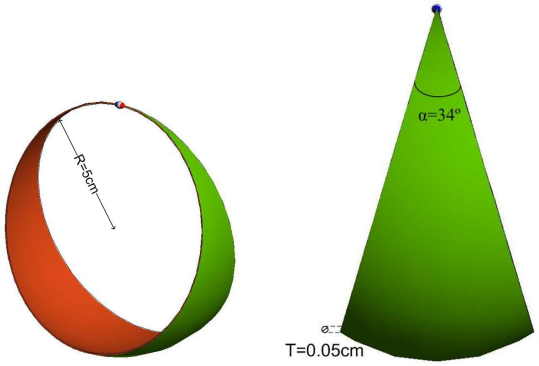

(a) Perspective view (b) Top wiew

Figure 4.29: Second candidate: original antenna dimensions

The feeding gap has been isolated since the beginning, and the best distance is 1mm. Nevertheless, the best dimensions for the isolated region will have to be checked, because it changes the behavior of the return loss in some frequencies.

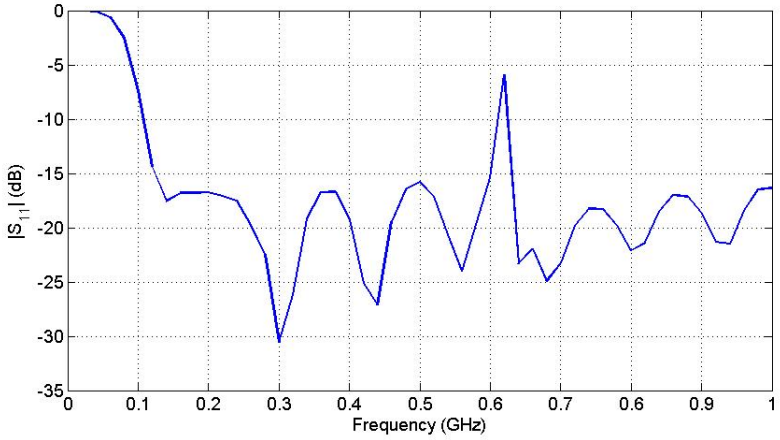

Figure 4.30: S_{11} of original second candidate

The results of the FEKO's simulation for this original shape indicate:

1. The return loss is less than -10dB from 110MHz (Figure 4.30).

2. The behavior is UWB because the bandwidth is greater than 500MHz (Figure 4.30). However, there is a peak at 620MHz that does not let to reach a larger bandwidth. With the parameters optimization it is expected to remove this peak.

4.3.1 Parametric study

The parametric study of the second candidate is presented, where the parameters to analyze are:

- Angle (α)
- Thickness (T)
- Feeding region

The original parameters are shown in Figure 4.29. These original values have been taken because they are similar of the typical bow-tie and loop parameters. The most suitable antenna will be found changing these values and comparing them to the original ones. The size is not taken into account because, as it has been checked in the study of the first candidate, the variation of the radius only changes the frequency range where the antenna is matched. Thus, the size of the shape will depend on the application requirements.

Angle

The first angle tested in the parametrization has been $\alpha = 34°$. Results presented in Figure 4.31a show that there are better angles. Actually, the angle that allow the greatest bandwidth without peaks is $\alpha = 24°$.

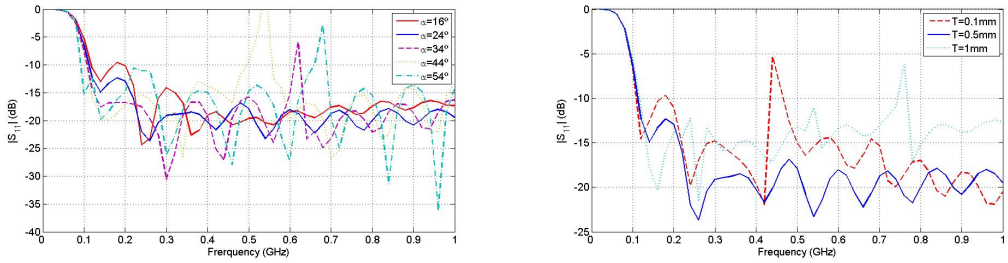

(a) Angle (b) Thickness

Figure 4.31: $|S_{11}|$ of the second candidate changing some parameter

Thickness

Another parameter to be analyzed is the thickness of the antenna. Three different values have been tested and Figure 4.31b shows the results. The best value is T=0.05cm,

because the return loss does not have peaks above -10dB. The other values have a behavior with a lot of irregularities and peaks.

Feeding region

The feeding split is 1mm because the region is isolated from the water, as it has been seen in last sections. Nevertheless, the dimensions of the isolated region where the feeding is placed can be modified to improve the return loss level (Table 4.3).

Table 4.3: Tested dimensions (in cm) of the air region to isolate the feeding

Case	Width (FW)	Depth (FD)	Height (FH)
Original one	0.1	0.2	0.15
First case	0.2	0.4	0.2
Second case	0.4	0.8	0.3
Third case	0.8	1.6	0.4

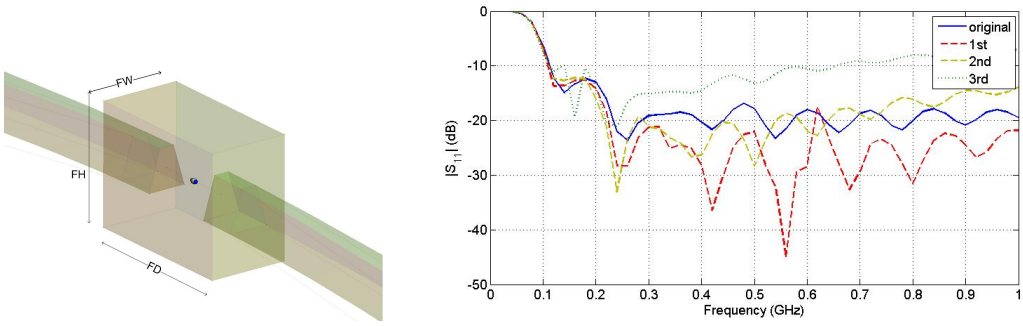

(a) Studied parameters of the isolated region

(b) S_{11} of the different sizes of the isolated region ($\alpha = 24°$)

Figure 4.32: Isolated region of the second candidate

Figure 4.32b shows the results of the four sizes tested for the antenna with an angle $\alpha = 24°$. It can be observed that the best options are the first case or the second case. In next sections both cases will be studied with internal isolation.

Final dimensions

The result of the parametrization of this antenna is a folded bow-tie antenna with the dimensions shown in the Figure 4.33. Notice that the feeding region has two options, the first and the second case studied in last section.

The return loss is shown in Figure 4.34, and the radiation pattern in Figure 4.35 (the radiation pattern of both cases is almost the same).

The results of the FEKO's simulation indicate:

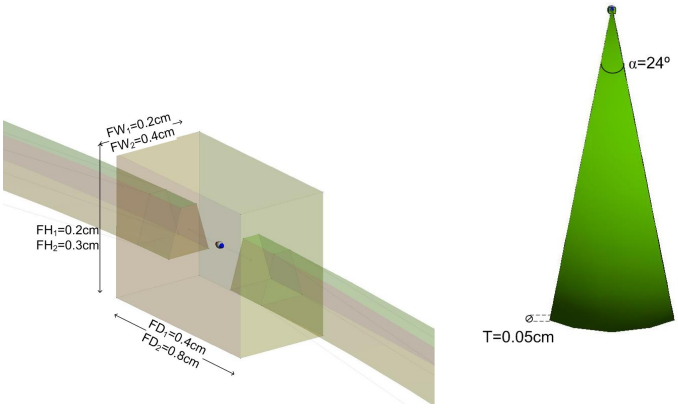

(a) feeding region (b) profile view

Figure 4.33: Dimensions of the final antenna

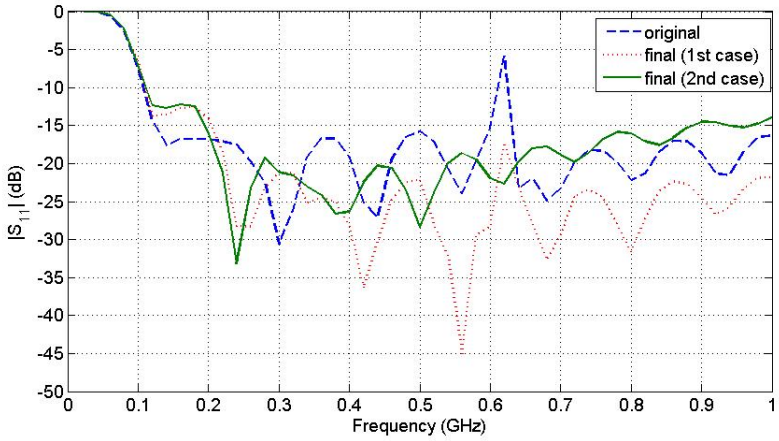

Figure 4.34: S_{11} of the new antenna and the old one

1. In both cases the return loss is less than -10dB from 110MHz (Figure 4.34), the same frequency as the original one.

2. The peak at 620MHz with a level above -10dB has been removed. Actually, in the second case any peak in this frequency cannot be found, while in the first case there is a peak below -10dB.

3. The behavior is UWB because the bandwidth is greater than 500MHz, it is from 110MHz to more than 1GHz.

4. In Figure 4.35 indicates that the radiation pattern is almost omnidirectional, specially in the frequencies close to 150MHz. However, in higher frequencies, it

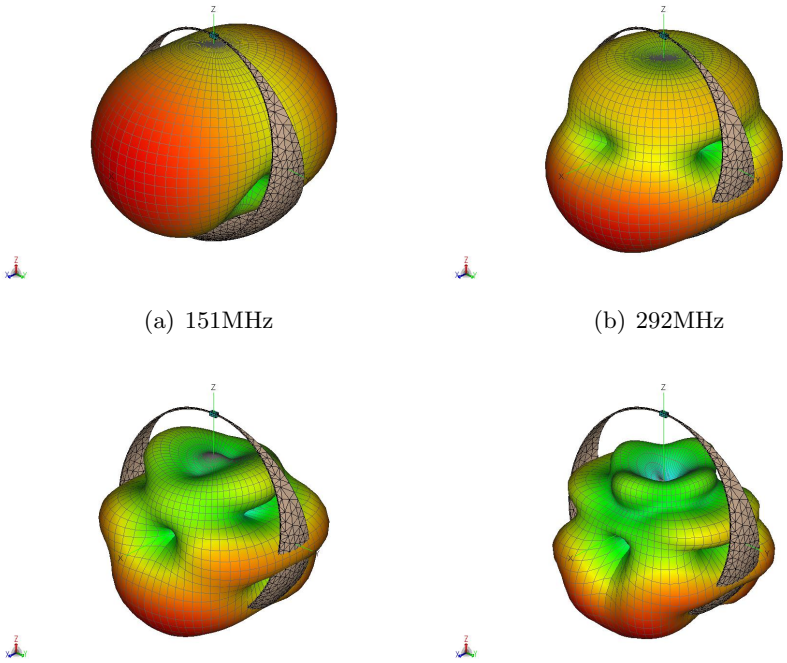

(a) 151MHz (b) 292MHz

(c) 454MHz (d) 596MHz

Figure 4.35: Radiation pattern of the second candidate without internal isolation

is not totally omnidirectional because when the length of the ring is greater than a half-wave dipole, some new nulls and some new lobes in the pattern appear.

4.3.2 Final shape with internal isolation

The isolation of the antenna's center has been done at the same way as the first candidate (Figure 4.36).

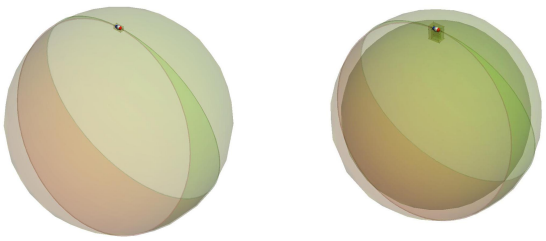

(a) air ball (b) air-teflon ball

Figure 4.36: Second candidate with internal isolation

The solution consists of placing an air sphere or an air-teflon (teflon has an ε_r of 2.1) sphere in the middle of the final shape with the improved dimensions. The changes in the behavior of the two final cases of this antenna will be studied.

Return loss

Figure 4.37 shows the $|S_{11}|$ results of the three models proposed of the second antenna candidate: the antenna without internal isolation, with an air ball, and with an air-teflon ball. Two sizes of the feeding region are tested:

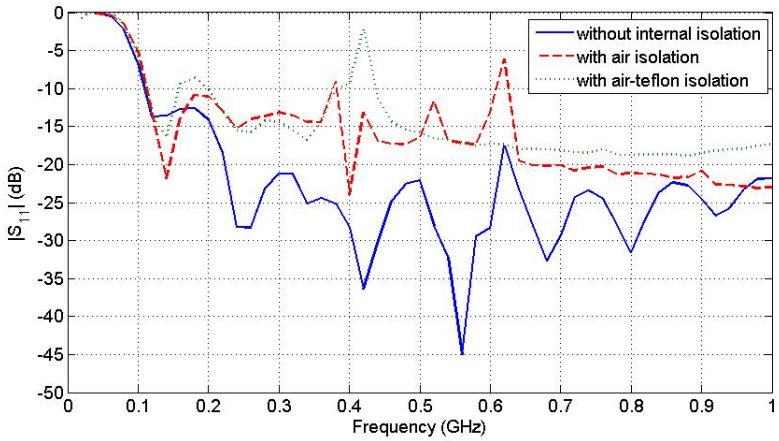

(a) 1st case of feeding region dimensions

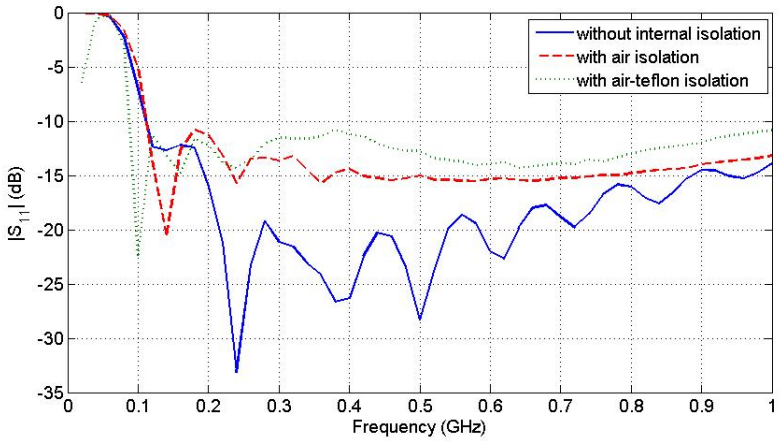

(b) 2nd case of feeding region dimensions

Figure 4.37: S_{11} of the two cases of the second candidate with and without internal isolation

- In the first case, the first thing that can be noticed is that the return loss level

starts to be lower than -10dB in the same frequency (110MHz) in the three antennas (with and without internal isolation). However, when there is internal isolation, there are some frequencies with a level higher than -10dB, specially in the case of the air-teflon sphere. This bad behavior is due to the effect of the isolated region in the feeding. If some parameters of the rectangular region where the feeding is placed are changed better results can be obtained.

- In the second case, it can be seen that the return loss level does not have any peak above -10dB in the three curves. It can also be observed that when an air-teflon ball is placed as internal isolation, the $|S_{11}|$ level starts to be less than -10dB before than the other cases, at 90MHz. This is a good result because, as far as we know, the propagation of electromagnetic waves in water is better with the lowest possible frequencies.

Therefore, it can be concluded that the best shape in this antenna's candidate is the second case of the feeding region (Figure 4.37b) where the dimensions were shown in Figure 4.33a (FW=0.4cm, FD=08cm, FH=0.3cm). The three models are UWB with a bandwidth greater than 900MHz, but with the internal isolation the return loss level is close to -10dB. However, it is not a problem while it was lower than this value because it means that more than the 90% of the power is transmitted.

Radiation Pattern

The best dimensions for the second antenna candidate have already been chosen and the return loss level of it has been analyzed. Now it is also important to study the 3D radiation pattern in some frequencies to check if it is omnidirectional or not.

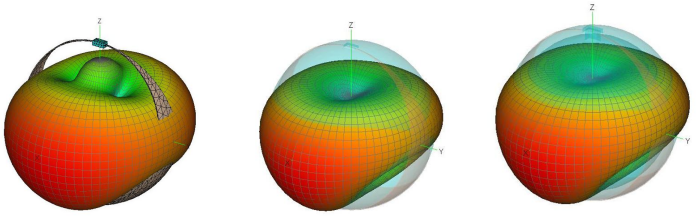

(a) without internal isolation (b) with air isolation (c) with air-teflon isolation

Figure 4.38: 3D radiation pattern at 191MHz

As Figure 4.38,4.39 and 4.40 show, the behavior of the radiation pattern in each case is totally different:

- At low frequencies (over to 200MHz) the radiation pattern of the three models are almost the same. The pattern is omnidirectional in the XY plane. In the model without internal isolation it is possible to observe that a secondary lobe

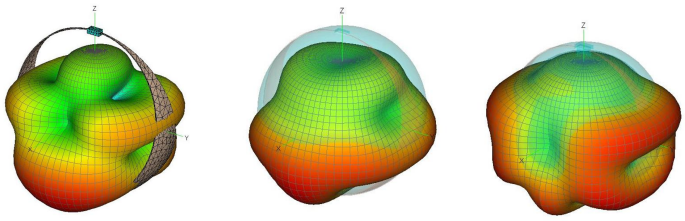

(a) without internal isolation (b) with air isolation (c) with air-teflon isolation

Figure 4.39: 3D radiation pattern at 393MHz

appears in the top of the shape. In the other patterns that does not occur because the permittivity in the center of the antenna is different, and it changes the wavelength of the radiate waves. The lobes appear when the length of the ring of the antenna is greater than a half-wave dipole.

- At medium frequencies (over to 400MHz) the pattern is different in each case. In the first model, the intensity of the signal is transmitted mostly in the bottom of the shape. In the second one, the transmission is done mostly in the bottom and in the middle. Finally, in the third case, the antenna radiates mostly of the power in the middle of the antenna (XY plane). In addition, when the antenna has internal isolation, the pattern is more omnidirectional because there are less lobes due to the smaller length of the wavelengths.

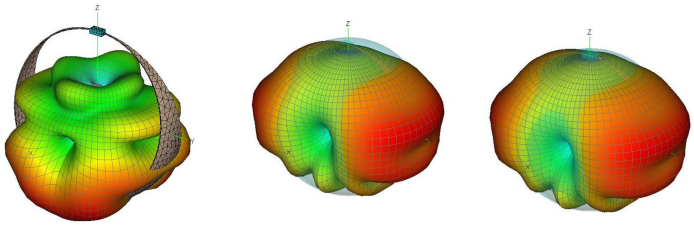

(a) without internal isolation (b) with air isolation (c) with air-teflon isolation

Figure 4.40: 3D radiation pattern at 596MHz

- At high frequencies (over 600MHz) the first model is very different of the other models. It radiates mostly of the energy in the bottom while, when there is internal isolation, the main lobes are in the middle and in the top of the antenna. In addition, when the antenna has internal isolation, the pattern is more omnidirectional because there are less lobes than the first model.

It can be also analyzed the radiation pattern in two dimensions in XZ plane (Figure 4.41) to study the behavior of the radiation pattern from another point of view.

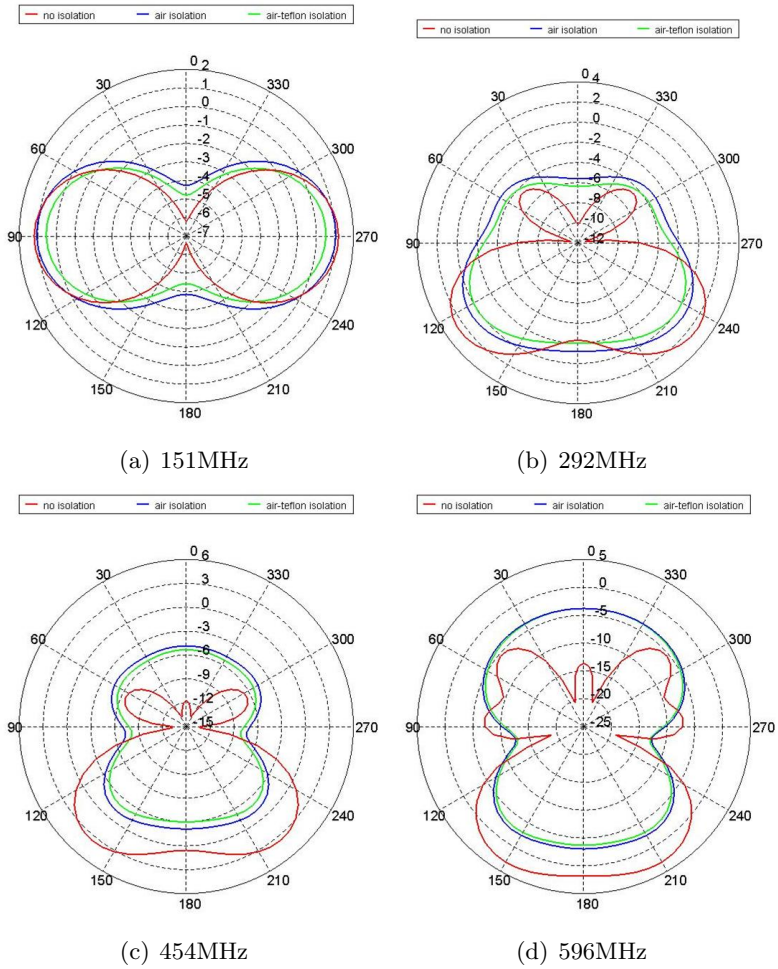

(a) 151MHz (b) 292MHz

(c) 454MHz (d) 596MHz

Figure 4.41: Radiation pattern of the gain (in dB) in 2D (XZ plane) at different frequencies

Finally, it can be concluded that the three models of the second antenna candidate are almost omnidirectional because when the antenna will be placed in a liquid medium, it will be floating, moving and rotating all the time. The results indicate that also in this case almost all the values of the gain are between -10dB and 0dB.

Directivity

Finally, an analysis of the directivity in dependance of the frequency in some directions is presented.

As it can be noticed in the results of Figure 4.43:

- The antenna without internal isolation has the maximum of transmission in the middle 1 (X direction) at low frequencies (from 90MHz to 240MHz) Otherwise, at

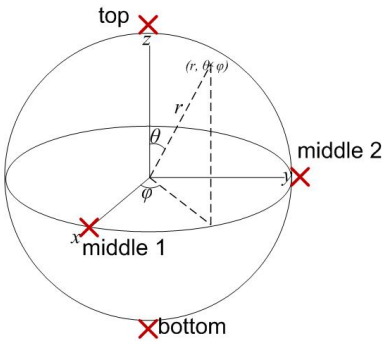

Figure 4.42: Spherical coordinates and points of interest

frequencies from 240MHz the mostly part of the energy is radiated in the bottom. The radiation in the middle 2 (Y direction) and in the top (Z direction) is not really good because the directivity oscillates in dependance of the frequency.

- In the cases of air and an air-teflon isolation, the radiation is higher in the middle 1 at low frequencies (from 90MHz to 250MHz in the model with air, and from 90MHz to 220MHz in the model with air-teflon). In the next 100-150MHz the direction with more radiation intensity is the bottom (-Z direction), and finally from 380Mhz the middle 2 (Y direction) has the higher directivity. In these cases with internal isolation, the top of the antenna (Z direction) and the middle 2 (Y direction) have also a curve with some oscillations, but not as sharp as the antenna without isolation. Notice that in high frequencies (from 500MHz) the directivity in the middle 1 (X direction) is very low, about -10dB.

It is also interesting to realize that almost all the level of the directivity is between -10dB and 5dB. If the radiation pattern was totally omnidirectional, the directivity would be 0dB in all the directions (like a perfect sphere). Otherwise, if the radiation pattern was directional, the directivity would be more than 0dB in some directions and less than 0dB in the rest of the pattern. Hence it can be concluded that the directivity of this antenna is different in each case and in each direction. Nevertheless, because of the continuous movement of the device where the antenna will be placed, the behavior is quite correct.

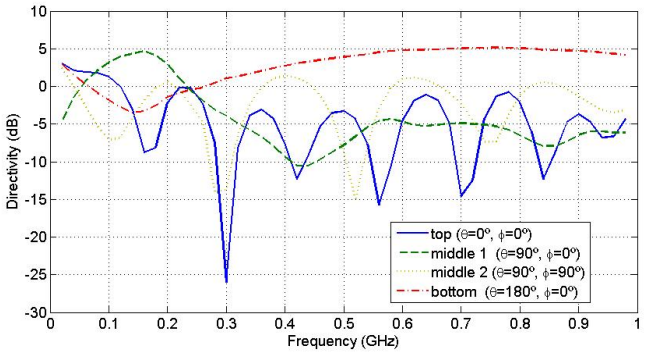

(a) antenna without internal isolation

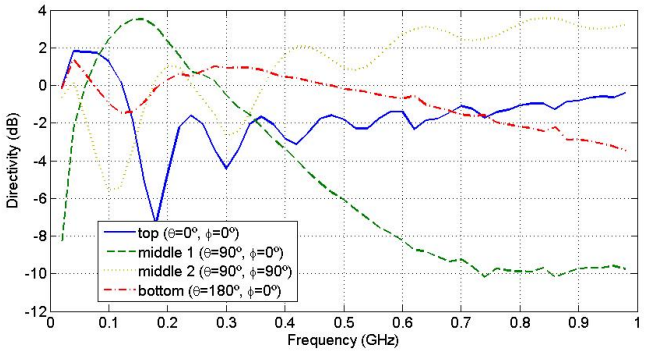

(b) antenna with air isolation

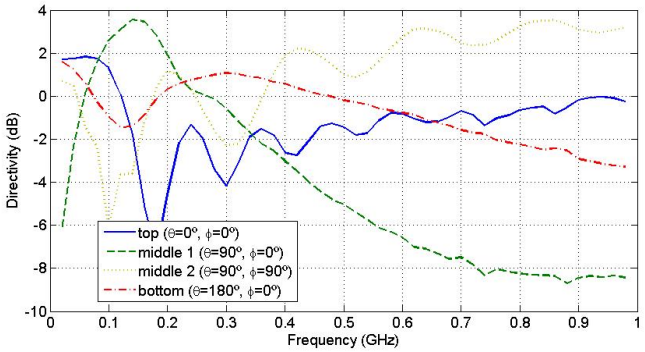

(c) antenna with air-teflon isolation

Figure 4.43: Directivity in dependance of the frequency

4.4 Folded Bow-tie Antenna: Third shape

Finally, the shape of the third candidate is presented. It is also a folded bow-tie loop antenna with the angle chosen on the side (as Figure 4.44b shows), but now the antenna is not a loop. This is the main difference from the second candidate.

In the beginning of the design of this new candidate, the same dimensions that the second antenna candidate have been chosen, but cutting the bottom of it.

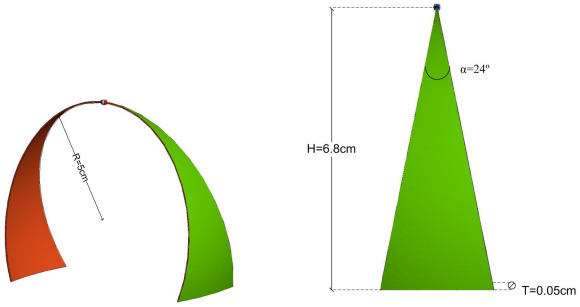

(a) Perspective view (b) Top wiew

Figure 4.44: Third candidate: original antenna dimensions

The feeding gap has been isolated since the beginning, and the best distance is 1mm. Nevertheless, the best dimensions for the isolated region will have to be checked, because it changes the behavior of the return loss in some frequencies.

The results of the FEKO's simulation for this original shape indicate:

1. The return loss is less than -10dB from 380MHz (Figure 41) because there is a peak between 300MHz and 400MHz above -10dB. If it was possible to remove it with the parametrization, the return loss would be less than -10dB from over 200MHz.
2. The behavior is UWB because the bandwidth is greater than 500MHz (Figure 4.45).

4.4.1 Parametric study

In the third antenna candidate, the parameters to improve are:

- Angle (α)
- Hight (H)
- Thickness (T)
- Feeding region

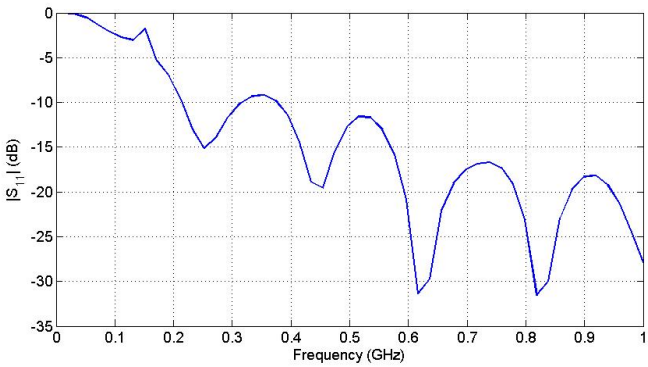

Figure 4.45: S_{11} of original third candidate

The dimensions of the original parameters are shown in Figure 4.44. These values have been taken because are similar of those of the second candidate. Changing them the behavior of the antenna for the requested application will be improved. The size is not taken into account because, as it was seen in the study of the first candidate, the variation of the radius only changes the frequency range where the antenna is matched. Thus, the size of the shape will depend on the application requirements.

Angle

As it can be noticed in Figure 4.46, there are other angles better than $\alpha = 24°$. These ones are $\alpha = 34°, \alpha = 44°$ and $\alpha = 54°$. Initially it has been taken an angle of 34° as the best candidate to test the parametrization of the next parameters.

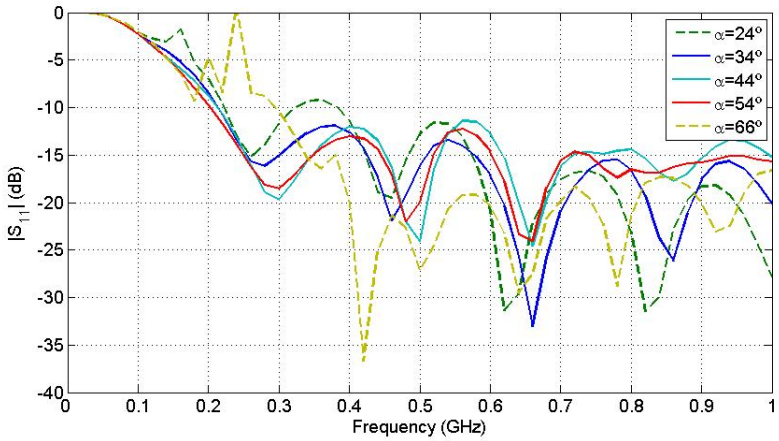

Figure 4.46: $|S_{11}|$ of the third candidate with different angles

Height

After finding a good angle, another parameter interesting to test is the height of the antenna (H). Figure 4.47a shows that a height of 7.5cm allows the antenna to transmit at lower frequencies.

Thickness

The thickness of the shape is also to be checked. Figure 4.47b indicates that the original thickness of 0.05cm is the best one, because the other tested ones have a $|S_{11}|$ level above -10dB in some frequencies.

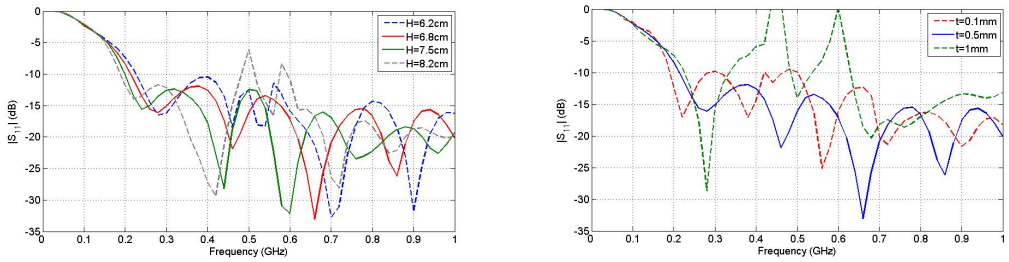

(a) Height

(b) Thickness

Figure 4.47: $|S_{11}|$ of the third candidate changing some parameters

Feeding region

The gap of the feeding is 1mm because the region is isolated from the water and this is the best distance. On the other hand, as it was observed in the second candidate, the region of the feeding has an important effect on the return loss. In this section three different sizes will be tested for that region apart from the original one to find the best dimensions, as it can be noticed in Table 4.4.

Table 4.4: Tested dimensions (in cm) of the air region to isolate the feeding

Case	Width (FW)	Depth (FD)	Height (FH)
Original one	0.1	0.2	0.15
First case	0.2	0.4	0.2
Second case	0.4	0.8	0.3
Third case	0.8	1.6	0.4

Indeed, as it can be seen in Figure 4.48b, the first and the second candidates for this region of isolation are also good for our purpose. To choose the best one, the viability to fabricate it is to be considered. That is the reason why the second one is chosen, because it will be easier to fabricate a big air region in the feeding.

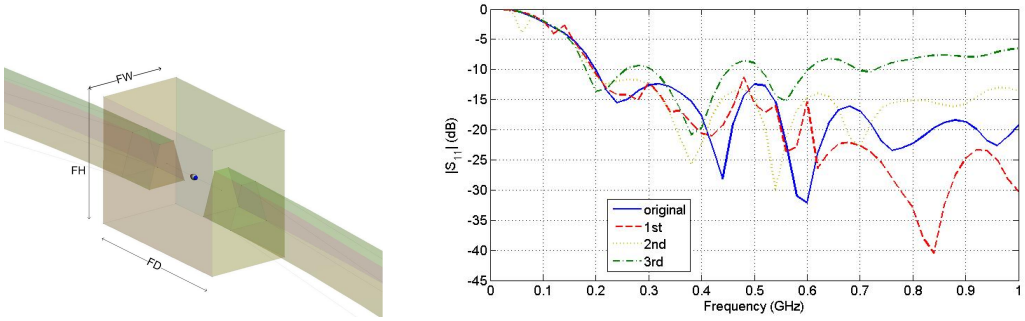

(a) Studied parameters of the isolated region

(b) S11 of the different sizes of the isolated region

Figure 4.48: Isolated region of the third candidate

Final dimensions

The result of the parametrization of this antenna is a folded bow-tie antenna with the dimensions shown in the Figure 4.49.

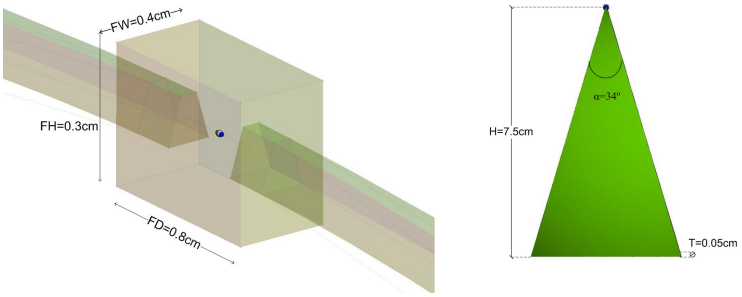

(a) feeding region

(b) profile view

Figure 4.49: Dimensions of the final antenna

The return loss is shown in Figure 4.50, and the radiation pattern in Figure 4.51. The results of the FEKO's simulation indicates:

1. The return loss is less than -10dB from 180MHz (Figure 4.50), a frequency lower than the original one.
2. The peak between 300MHz and 400MHz with a level above -10dB has been removed.
3. The behavior is UWB because the bandwidth is greater than 500MHz, it is from 180MHz to more than 1GHz.

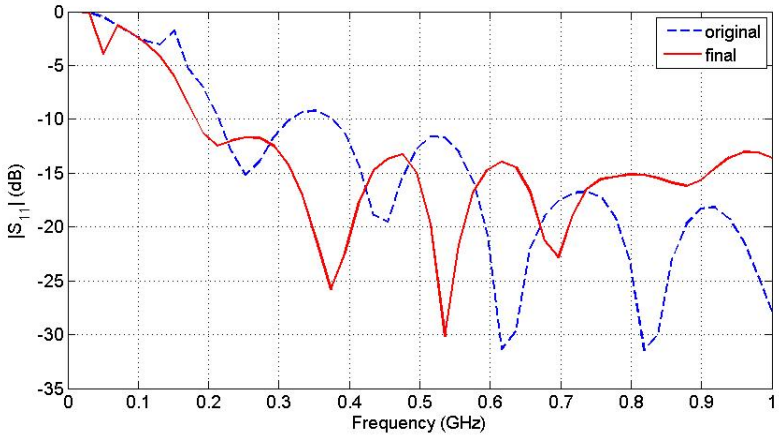

Figure 4.50: S_{11} of the new antenna and the old one

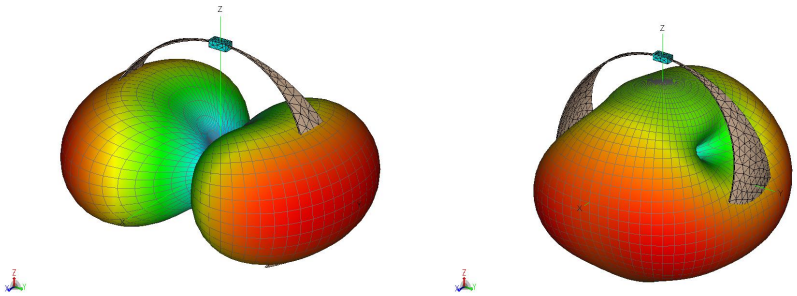

(a) 192MHz

(b) 292MHz

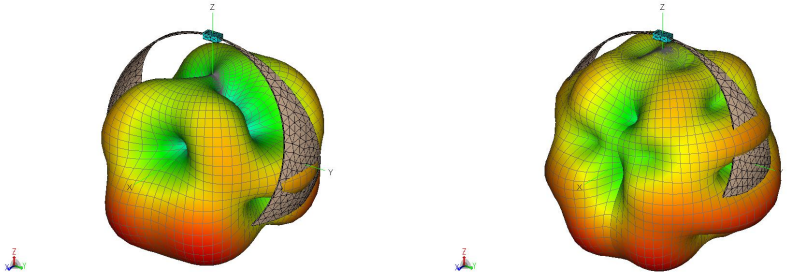

(c) 454MHz

(d) 596MHz

Figure 4.51: Radiation pattern of the third candidate without internal isolation

4. As it can noticed in Figure 4.51, the radiation pattern is almost omnidirectional, specially in the frequencies close to 200MHz. However, in higher frequencies, it is not totally omnidirectional because when the length of the ring is greater than a half-wave dipole, some new nulls and some new lobes appear in the pattern.

4.4.2 Final shape with internal isolation

As in the first two candidates, an air or air-teflon sphere is put inside the antenna to isolate the battery and the electrical circuit from the water (Figure 4.52). This isolation ball implies important changes in the behavior of the antenna, hence an analysis of these variations is presented in this section.

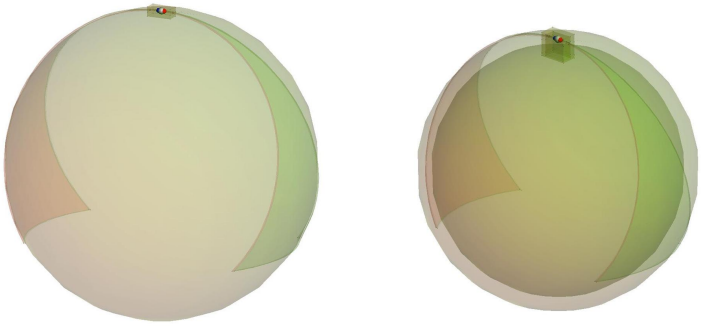

(a) air ball (b) air-teflon ball

Figure 4.52: Second candidate with internal isolation

Return loss

First, we test the return loss level of the three models: without internal solation, with an air ball, and with an air-teflon ball.

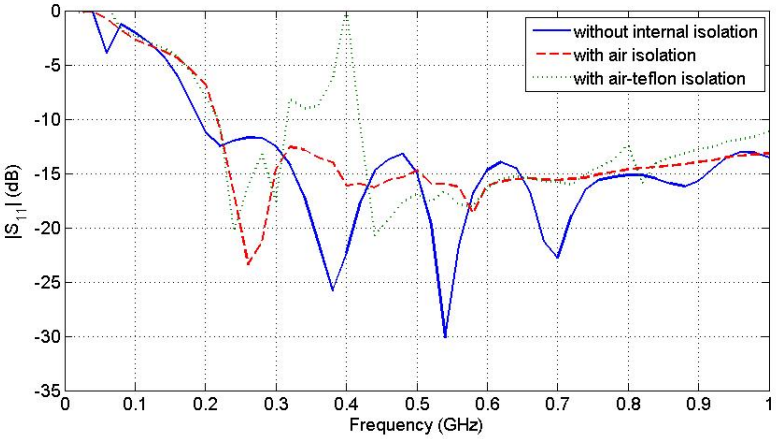

(a) 1st case of feeding region dimensions

Figure 4.53: S_{11} of the third candidate with and without internal isolation

The results of the Figure 4.53 indicate the antenna works in a good way with the internal air ball, but not with the internal air-teflon ball. The problem in the third

model is a great peak in the range of frequencies between 310MHz and 410MHz. To remove it there are some solutions: changing the feeding air region (Figure 4.49a), changing the teflon for another kind of plastic, tapering the ends of the antenna...etc. Another possibility is that the FEKO simulation has to be done with a more accurately mesh. However, quite a lot of proofs have been done without finding good results.

If it is considered the first frequency with a return loss level below -10dB as a very important request, it can be seen this shape is worse than the other two candidates, because this frequency is close to 200MHz. This is the reason why this shape has been considered as the worst one of the three candidates. Nevertheless, an analysis of its characteristics is presented in this section, because the model with the air ball isolation has a correct response. In that case the return loss is matched from 210MHz, and from 320MHz it has a planar behavior close to the -15dB.

Radiation Pattern

After to check the return loss, the analysis of the radiation pattern in some frequencies is presented.

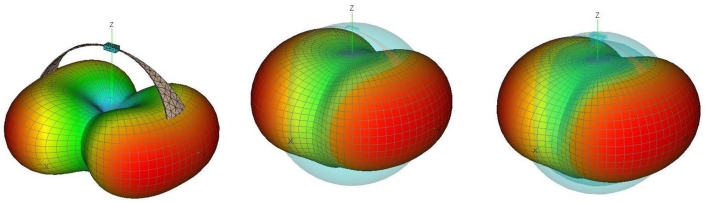

(a) without internal isolation (b) with air isolation (c) with air-teflon isolation

Figure 4.54: 3D radiation pattern at 212MHz

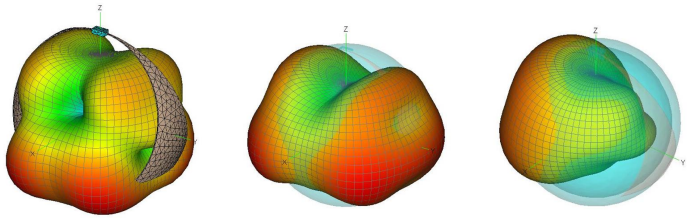

(a) without internal isolation (b) with air isolation (c) with air-teflon isolation

Figure 4.55: 3D radiation pattern at 393MHz

Figures 4.54,4.55 and 4.56 show the results in 3D, while Figure 4.57 shows the radiation pattern in 2D (XZ plane). It can be observed that:

- At low frequencies (over to 200MHz) the pattern is omnidirectional in the XY plane.

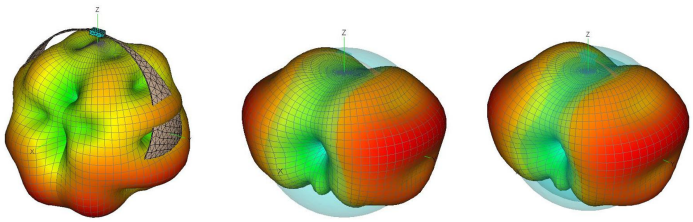

(a) without internal isolation (b) with air isolation (c) with air-teflon isolation

Figure 4.56: 3D radiation pattern at 596MHz

- At medium frequencies (over to 400MHz) the radiation of the first model is mostly in the bottom, while in the model with the air ball is almost of all in the bottom and in the middle. In the third case it is obtained a radiation pattern totally unusual because there is not a symmetry like in the others cases. Notice that in this frequency (393MHz) the return loss level of this third model was above -10dB.

- At high frequencies (over 600MHz) the first model has a lot of lobes, and the energy is concentrated in the bottom of the antenna. The radiation pattern of both models with internal isolation are similar, and they have a behavior quite omnidirectional, with a maximum of transmission in the middle of the sides.

The results indicate that also in this case almost of the values of the gain are between -10dB and 0dB.

Finally, it can be concluded that the the model without internal isolation and the model with internal air isolation radiates correctly in almost all the directions. When the antenna will be placed in a liquid medium, it will be floating, moving and rotating all the time. The results indicates that also in this case almost of the values of the gain are between -10dB and 0dB.

However, the third model (air-teflon isolation) has not an omnidirectional behavior in all the frequencies.

Directivity

The last parameter to analyze is the directivity in dependance of the frequency. In Figure 4.58 it can be observed the directions that have been studied.

In that case only the two first models have been studied (antenna without internal isolation, antenna with air inside) because the results of the third one do not have any utility. As it can be noticed in Figure 4.59, the graphic indicates:

- The antenna without internal isolation has the maximum of transmission in the middle 2 (Y direction) at low frequencies (from 90MHz to 240MHz) Otherwise, at frequencies from 240MHz the mostly part of the energy is radiated in the bottom

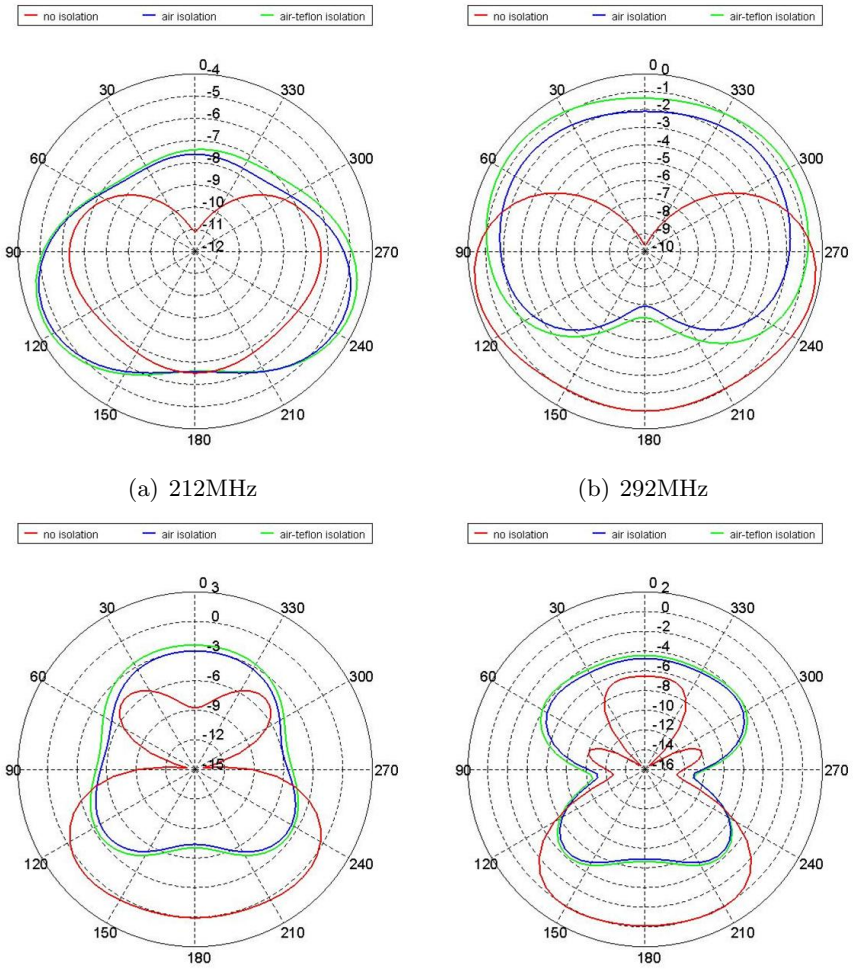

(a) 212MHz (b) 292MHz

(c) 454MHz (d) 596MHz

Figure 4.57: Radiation pattern of the gain (in dB) in 2D (XZ plane) at different frequencies

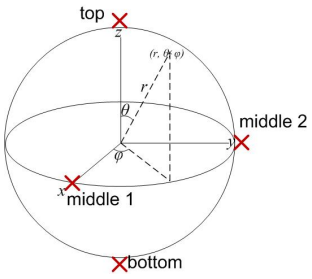

Figure 4.58: Spherical coordinates and points of interest

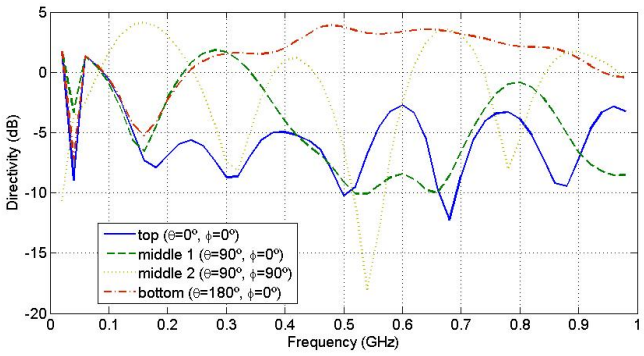

(a) antenna without internal isolation

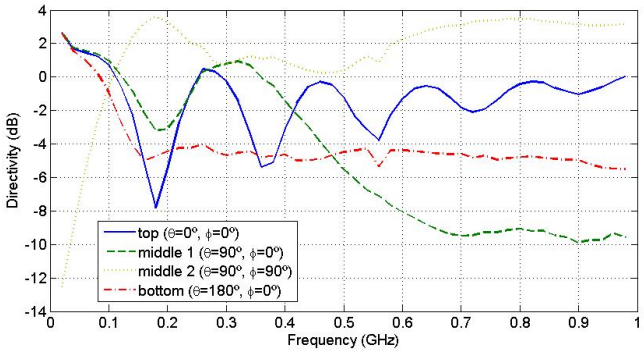

(b) antenna with air isolation

Figure 4.59: Directivity in dependance of the frequency

and in the middle 1 (this one only until 310MHz). The oscillations in the curves indicate that the behavior of the radiation is inadequate.

- In the case of air, the radiation is higher in the middle 2 in all the range of frequencies. There are oscillations in the top that means a bad behavior of radiation. At high frequencies (from 500MHz) the radiation in the middle 1 direction is so poor.

It is also interesting to realize that, as in the other two candidates, almost all the level of the directivity is between -10dB and 5dB. The directivity depends on the frequency and the direction of radiation. However, the antenna will be in continuous movement, and this is the reason why it can be considered that the antenna has a correct radiation pattern in the cases without internal isolation and with an air isolation.

4.5 Comparison of the three candidates

After improving the dimensions of the three antenna candidates some interesting parameters have been studied to understand the behavior of the antenna in each case. It has been proved that finally there is more than one candidate that achieve the requirements. In this section the obtained results will be compared to discern which one is the most suitable candidate to satisfy the purpose of the application. The parameters to compare are the same that have been studied in last sections: return loss, radiation pattern, and directivity.

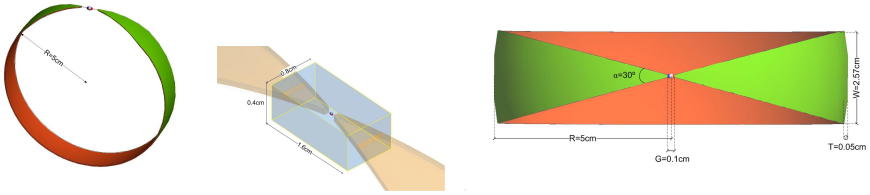

(a) 1st: perspective view (b) 1st: feeding region (c) 1st: top view

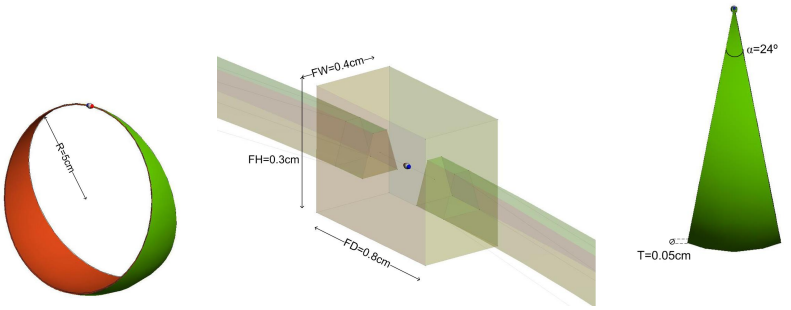

(d) 2nd: perspective view (e) 2nd: feeding region (f) 2nd: profile view

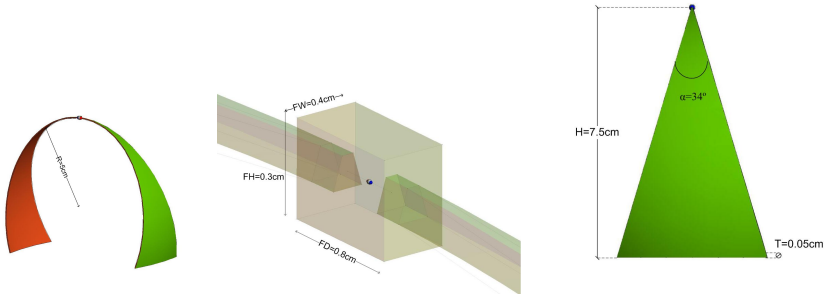

(g) 3rd: perspective view (h) 3rd: feeding region (i) 3rd: profile view

Figure 4.60: Final shapes of the three candidates without internal isolation

4.5.1 Final shapes

First, the three candidates without internal isolation are considered. Figure 4.60 reminds the dimensions of each shape.

Notice that all the shapes have a radius of 5cm. However, depending on the requirements, the antenna could be smaller, but the first frequency with a return loss level lower than -10dB would be higher.

Return loss

The most important parameter is the return loss. Without a good matching in the frequency range of interest, the antenna cannot be suitable for the application.

The guidelines to choose the best antenna are:

- A return loss less than -10dB as the lowest frequency as possible, because the electromagnetic waves in water propagate better in low frequencies.
- A large bandwidth, because the antenna has to work in a UWB network.

Following these two points, it can be concluded watching the Figure 4.61 that the best antenna is the second one, followed by the first one. The antenna with a worst return loss is the third candidate.

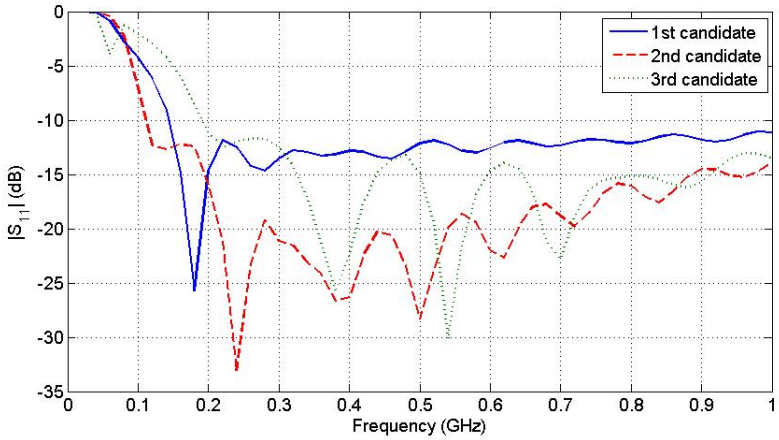

Figure 4.61: $|S_{11}|$ of the three candidates without internal isolation

Radiation Pattern

The radiation pattern is also very important because an antenna as omnidirectional as possible is preferred. The candidate which has the radiation pattern more similar to a sphere will be the best one. However, it has to be taken into account that the radiation pattern changes in dependance of the frequency.

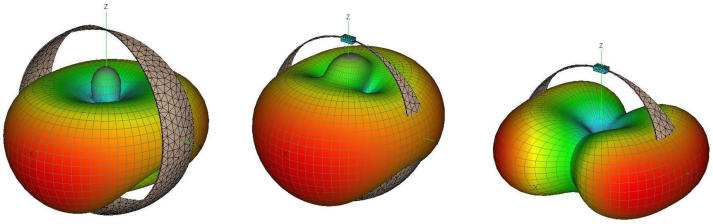

(a) 1st candidate (b) 2nd candidate (c) 3rd candidate

Figure 4.62: 3D radiation pattern at 200MHz

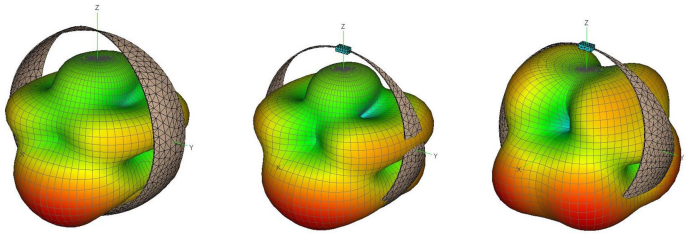

(a) 1st candidate (b) 2nd candidate (c) 3rd candidate

Figure 4.63: 3D radiation pattern at 400MHz

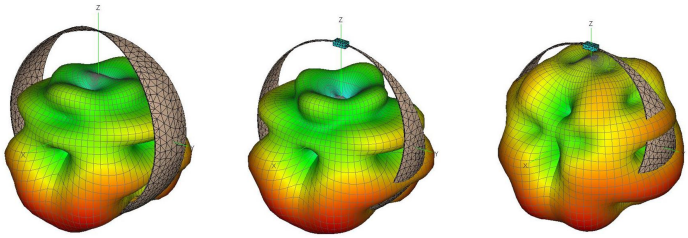

(a) 1st candidate (b) 2nd candidate (c) 3rd candidate

Figure 4.64: 3D radiation pattern at 600MHz

Figures 4.62, 4.63 and 4.64 show the radiation pattern of the three candidates at frequencies close to 200MHz, 400MHz and 600MHz:

- At low frequencies (200MHz), the pattern of the second candidate is really adequate. The first one is also quite good, and the third one is only omnidirectional in the XY plane.
- At medium frequencies (400MHz), the radiation pattern of the three candidates is more or less similar referred to the omnidirectionallity.
- At high frequencies (600MHz), the third model is the most suitable to radiate in all the directions, while the first and the second radiates more in the bottom than in the top.

Realizing these results, it has been also chosen the second shape as the best one in this issue, because at low and at medium frequencies its radiation pattern is very good.

Directivity

The last parameter that is taken into account to do the selection of the best candidate is the directivity, who will tell how does the radiation intensity change in dependance of the direction and the frequency.

As it can be noticed in Figure 4.65, the directivity of the first and the second candidates is almost the same, while the third one has some differences. However, the differences amongst them are not enough important to prioritize one candidate face up to the others.

Finally, after the comparison of these antenna candidates, it can be concluded that the best one is the second folded bow-tie antenna.

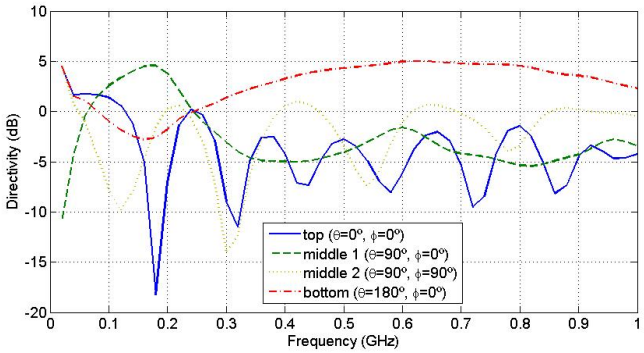

(a) 1st candidate

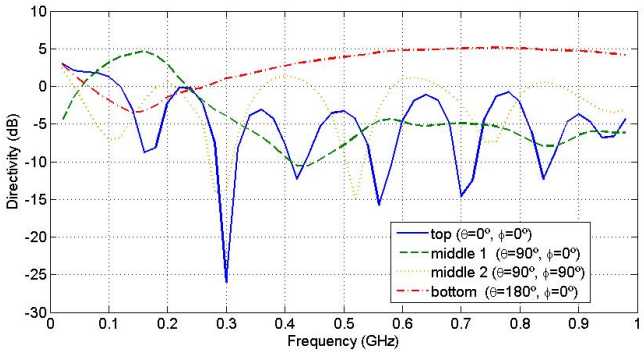

(b) 2nd candidate

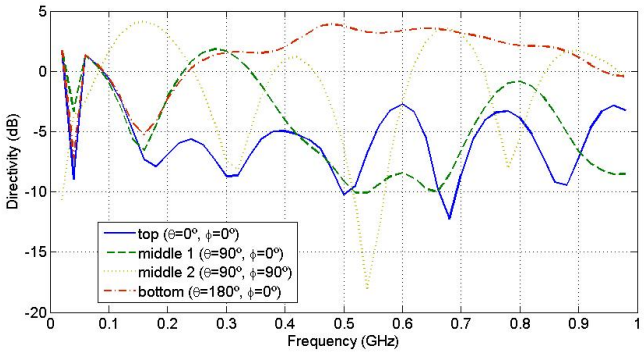

(c) 3rd candidate

Figure 4.65: Directivity in dependance of the frequency

4.5.2 Final shapes with internal isolation

Now, an internal isolation has been placed inside the antenna. As it can be observed in section 4.4.2, the air-teflon internal sphere produces a bad response in the third candidate. Furthermore, in the other shapes, the difference between the model with air and the model with air and teflon is not very significative. Thus, in this section the cases with only air isolation will be studied. To construct it, it has been taken the original shapes and it has been included the air ball inside, as in Figure 4.66.

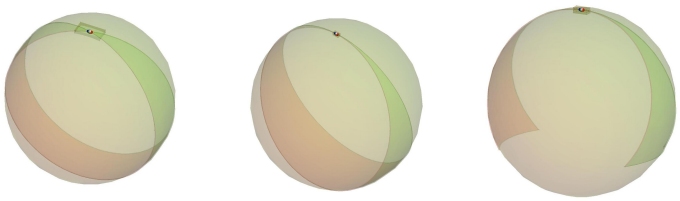

(a) 1st candidate (b) 2nd candidate (c) 3rd candidate

Figure 4.66: Candidates with internal air isolation

Return loss

Figure 4.67 allows to realize the differences among the shapes in the return loss level. It is possible to appreciate that the candidate with a better $|S_{11}|$ is the first one, because it starts to be lower than -10dB before the others and the level in low frequencies are lower than the others. The bandwidth of this candidate is shorter than the second and the third candidates, but it is enough because it is bigger than 500MHz, and it means that is an UWB behavior.

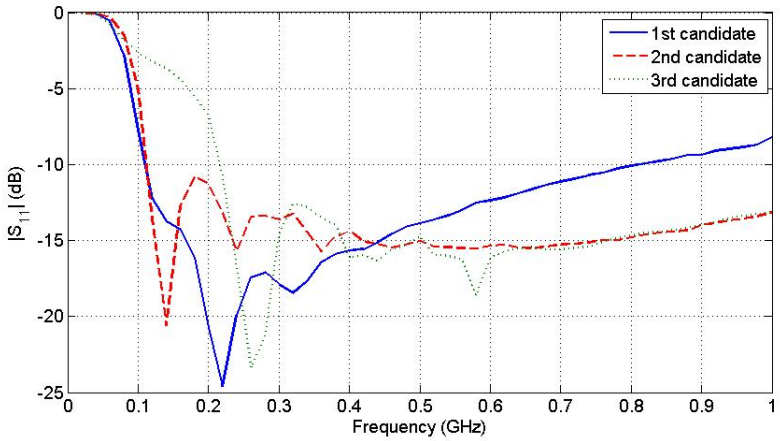

Figure 4.67: $|S_{11}|$ of the three candidates with internal air isolation

Radiation Pattern

The internal isolation of the candidates modifies the radiation pattern. As it can be checked in Figures 4.68,4.69 and 4.70, the first candidate is also the best, because in all the frequencies is more omnidirectional than the others.

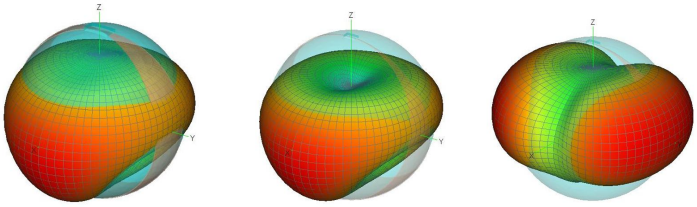

(a) 1st candidate (b) 2nd candidate (c) 3rd candidate

Figure 4.68: 3D radiation pattern at 200MHz

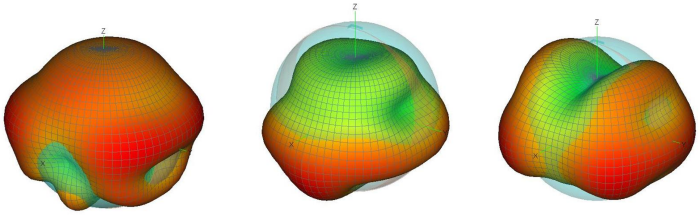

(a) 1st candidate (b) 2nd candidate (c) 3rd candidate

Figure 4.69: 3D radiation pattern at 400MHz

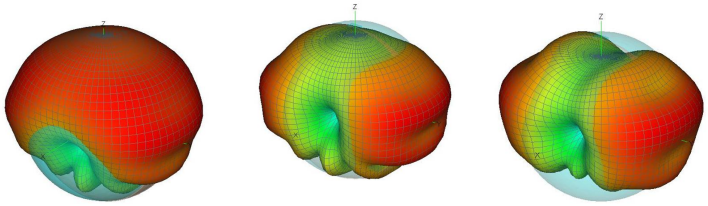

(a) 1st candidate (b) 2nd candidate (c) 3rd candidate

Figure 4.70: 3D radiation pattern at 600MHz

Directivity

Finally, Figure 4.71 shows the directivity of each candidate in dependance of the frequency and in four different directions. The characteristics of these curves do not contribute a lot to choose the best shape.

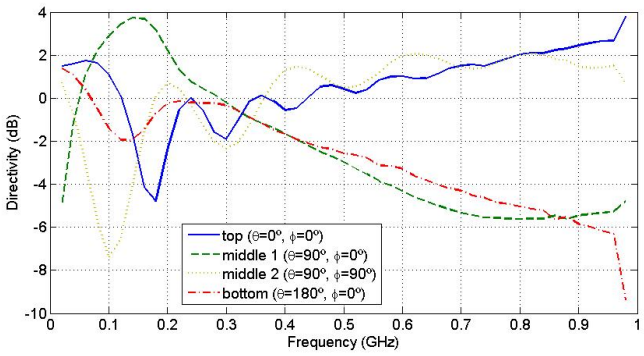

(a) 1st candidate

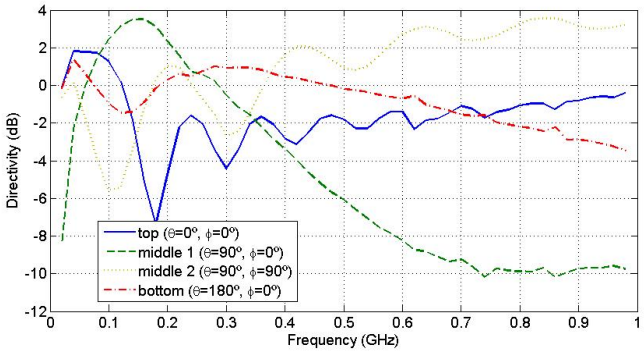

(b) 2nd candidate

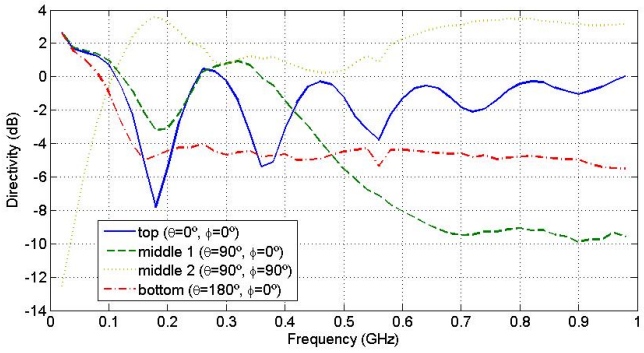

(c) 3rd candidate

Figure 4.71: Directivity in dependance of the frequency

Finally, it can be concluded that when the antenna has internal isolation for the battery and the electrical circuit, the best candidate is the first folded bow-tie antenna.

4.5.3 Conclusions

In this section it has been done an extensive study of the three antennas proposed for an underwater application. The dimensions have been improved till finding the best results in each case, and some important features of the antennas have been analyzed. After that, it has been concluded two main issues:

- The best candidate without internal isolation is the second one.
- The best candidate with internal isolation is the first one.

4.6 Variations in the medium

4.6.1 Conductivity

FEKO software provides some useful options to vary the parameters of the medium. One of these parameters is the conductivity, which has an important effect in return loss, as it has been seen in Section 2.2.1. After finding a good shape for the application in pure water ($\sigma = 0S/m$), other conductivities will be studied in the final design. Notice that all of these simulations have been done with a constant relative permittivity of 81.

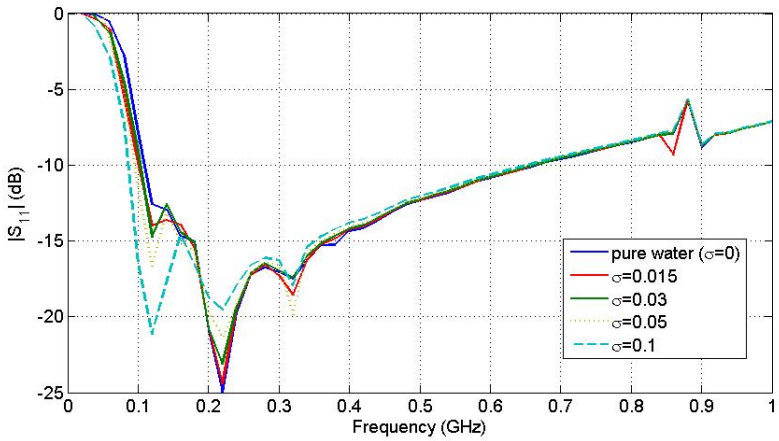

Figure 4.72: S_{11} of the final candidate with air-teflon isolation in different conductivities

Figure 4.72 shows the return loss of the final shape with air-teflon isolation with different conductivities. As it can be seen in Section 2.2.1, the usual conductivity values of water (not sea water) are below 0.1S/m. Watching the graph, it can be concluded that the level of return loss does not experiment a significative modification. Actually, the higher the conductivity is, the better the results at low frequencies are.

Conductivities higher than 0.1S/m have not been studied because, as it will be shown in next sections, the communications in water at these conductivity levels are not possible in distances of more than half a meter.

4.6.2 Permittivity

Another important issue to take into account when some communication is working in a liquid is the permittivity of the medium. Up to now it has only been studied the response if the antennas in water with a dielectric constant of 81. However, as it has been discussed in Section 2.2.2 (Figure 2.3), the permittivity of the water decreases with the temperature. In fact, at 0°C the $\varepsilon = 88$ and at 100°C, $\varepsilon = 50$. Thus, it is going to be studied the behavior of the final antenna with internal isolation in that range (ε from 50 to 88).

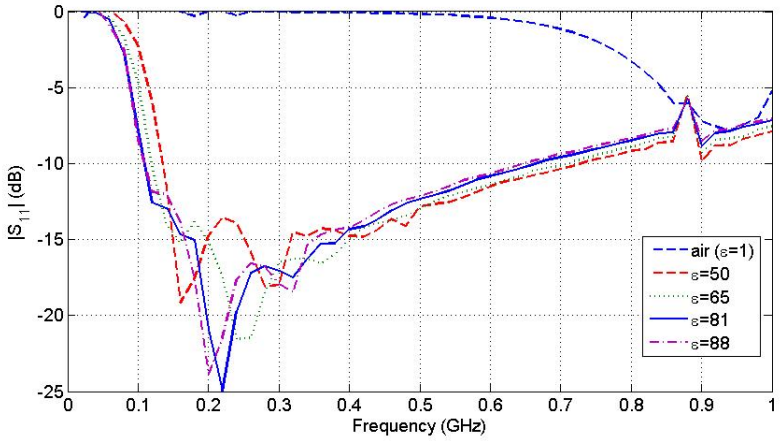

Figure 4.73: S_{11} of the final candidate with air-teflon isolation in different permittivities

As can be noticed in Figure 4.73, the return loss of the antenna in a medium with a permittivity between 50 and 88 does not change a lot. The main change is that in the case of the $\varepsilon = 50$ an unusual peak at 220MHz can be appreciated, due to the variation of the impedance. However, this level of this peak is minor than -10dB. It can be observed that the same antenna in air has a very bad behavior. That occurs because of the complete variation of the impedance. Thus, if it uses a liquid with a very low permittivity, the antenna will not work in a proper way.

4.6.3 Conclusions

In this section it has been analyzed the variations of the return loss level of the proposed antenna when some parameter of the medium changes. However, it has been checked that the antenna works good in those cases.

Specifically, in the typical values of the drinking water (σ from 0.015 to 0.05) the antenna works perfectly. In higher frequencies than 0.1, it will be seen in next sections that the channel attenuation is too high to establish good communications. Hence higher conductivities have not been tested in this section.

On the other hand, in a temperature of water between 0°C and 100°C, the permittivity varies from 50 to 88. The proposed antenna in these conditions has also a

good return loss level. However, at low permittivities (close to air), this antenna is not useful.

4.7 Transmission level and channel attenuation

Up to now it has been studied the return loss level ($|S_{11}|$), but it is also important to know the transmission level ($|S_{21}|$ or $|S_{12}|$) between two antennas to analyze the viability of a possible network with them. In addition, there are some elements which change the behavior of the channel attenuation, and they have to be analyzed too, to determine under which conditions our system will be able to work.

To do this study, it has been used a pair of dipoles with the same characteristics, because the folded bow-tie antenna requests too much computational resources to perform this study. Some FEKO simulations have been done, changing the distance between the dipoles and changing also the conductivity of the medium to compare the results.

4.7.1 Dipoles in air

First of all, we analyze the transmission level of the pair of dipoles in air to be able to check the differences in water. We have tried a 300MHz frequency because it is one of the most representative frequencies inside the bandwidth of the application.

In that case, the dipoles have a length of 0.5 meters ($\lambda = 1m$). If we take a look to an old Section (2.2.5), we can see that the work frequency is 300MHz (2.10). The $|S_{21}|$ has been studied between the two dipoles in a range of frequencies from 10MHz to 500MHz, and a distance from 10 centimeters to 3 meters.

As you can observe in Figure 4.74, the attenuation changes depending on the distance and on the frequency. The maximum transmission level is always around the work frequency of 300MHz, but the level in that frequency decreases with the distance.

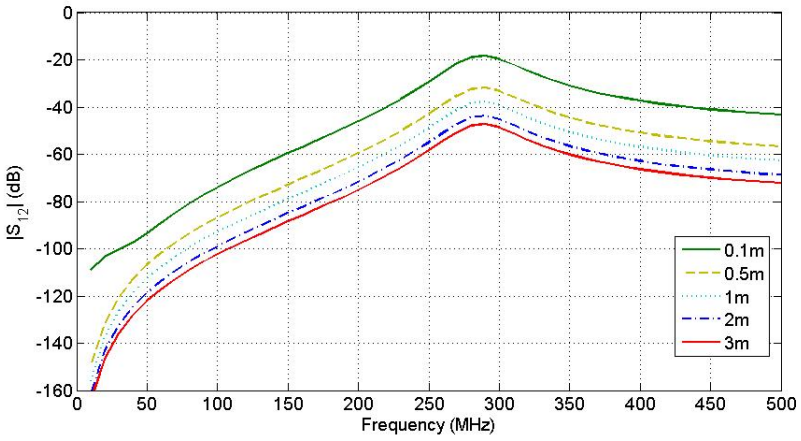

Figure 4.74: Transmission level between two dipoles in air, in different distances (in meters)

However, Figure 4.74 does not give a perfect idea about the effect of the distance in

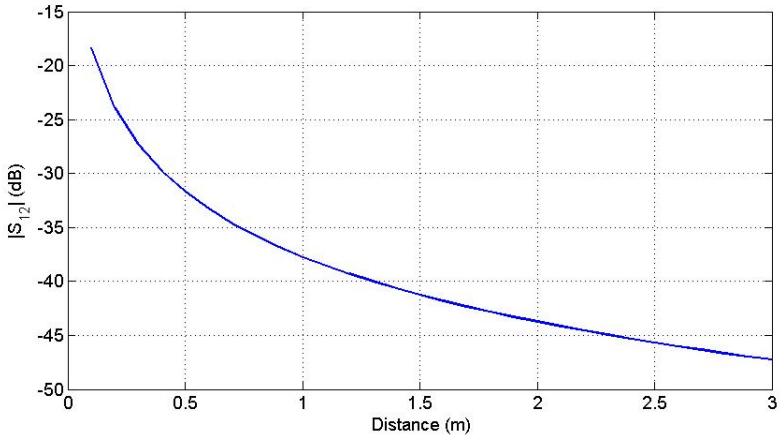

Figure 4.75: Transmission level between two dipoles in air at work frequency (300MHz), in different distances (in meters)

the attenuation. Otherwise, Figure 4.75 shows the transmission level between the pair of dipoles always at the same frequency (300MHz) but changing the distance. In that case it is easier to understand the behavior of the level's decrease. In a few centimeters of distance, the effect of the distance's increment in the transmission level is greater than in a longer distances.

4.7.2 Dipoles in water

As far as we know, the dimensions of the antennas in water can be 9 or 10 times smaller than in air with the same results. The reason for this is that we have taken a pair of dipoles of 6cm of length ($\lambda = 1/9 = 0.11m$) to study the transmission level in water and be able to compare the results.

The range of frequency taken into account for this simulation is the same one as the range in the last section (from 10MHz to 500MHz). We have chosen this range of frequencies because it is similar than the range of the interest for the underwater application that we are studying. The distances studied are also the same as the last section: from 10 centimeters to 3 meters.

In Section (2.2.1) the conductivity was presented of different kinds of water. A study of the transmission level of these different waters is presented.

Dipoles in pure water ($\sigma \approx 0$)

The two dipoles are placed now in an almost ultra pure underwater background, with a permittivity of 81 and a null conductivity.

From Figure 4.76 you can observe the behavior of the $|S_{12}|$ in water without conductivity. It depends of the frequency and the distance, and as we can see, the graphic

is different as the previous one in air. The main difference is that in water the transmission is not as narrow-band as in air.

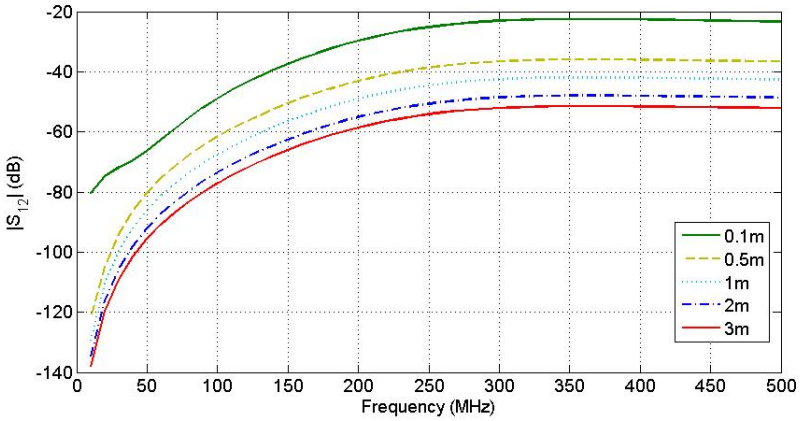

Figure 4.76: Transmission level between two dipoles in pure water, in different distances (in meters)

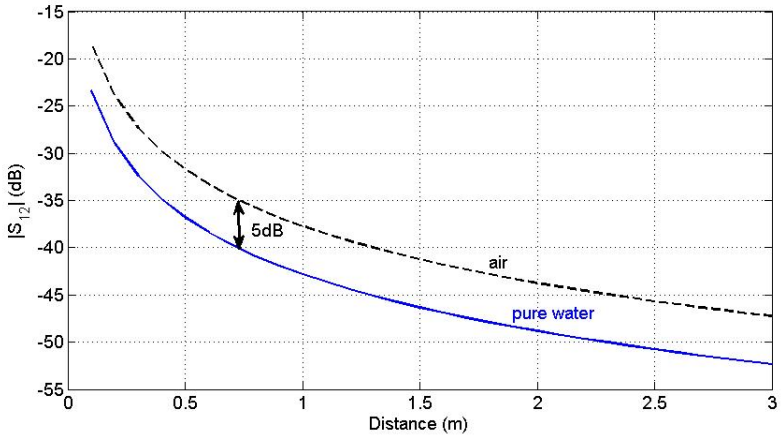

Figure 4.77: Transmission level between two dipoles at work frequency, in different distances (in meters)

Figure 4.77 shows that the difference of the transmission level in dependance of the distance between the air and the pure water is almost always 5dB. However, the trend of the curve is the same in both cases.

Dipoles in water with conductivity ($\sigma > 0$)

Now, an analysis of the transmission level in impure waters is presented. In Figure 4.78 and Figure 4.79 it can be checked that the $|S_{12}|$ decreases with the conductivity level.

Figure 4.78 shows the transmission level of the different kinds of water in 1 meter of distance between the two dipoles. In the Figure 4.79 it the transmission level has been taken into account at work frequency (300MHz) but in dependance of the distance.

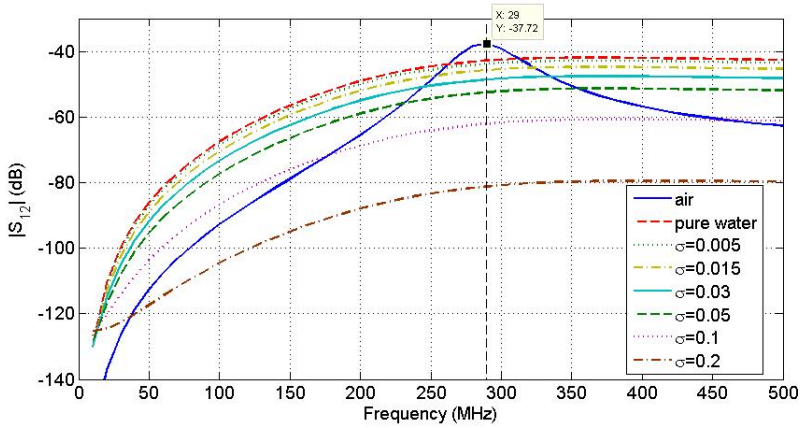

Figure 4.78: Transmission level between two dipoles in 1 meter of distance in impure water with different conductivities

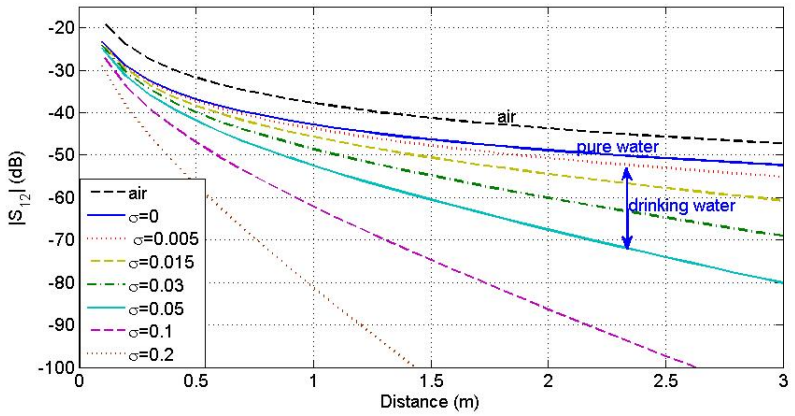

Figure 4.79: Transmission level between two dipoles at work frequency in water with different conductivities

In Figure 4.78 it is observable that when the conductivity is greater than 0.2S/m, the transmission level is too low to establish a good communication.

Furthermore, it is possible to see in Figure 4.79 that in small distances the attenuation level is not as different as in high distances, where the transmission level experiments a huge decrease in high conductivities.

4.7.3 Conclusions

In this section it has been studied the transmission level between two dipoles in different mediums (air, pure water, impure water).

It has been concluded that in water the attenuation is greater, specially in waters with an impurity superior than common drinking waters (0.05S/m). Moreover, the distance is very important to determinate if the communication between two antennas is suitable or not. Thus, there are two important factors to take into account in an underwater transmission: the conductivity of the medium and the distance between the antennas.

Chapter 5

Conclusions and future work

In this thesis an antenna for UWB underwater applications has been designed. In order to understand the goal of the thesis, first it has been given an overview of the characteristics of UWB technology, underwater propagation and classes of suitable antennas for our application. Two software tools have been analyzed to find out which one is the most suitable for underwater applications. Some antennas have been analyzed with FEKO software to find a shape for our application. The behavior of two of these antennas (loop and bow-tie) in water has proven to be a good beginning to the design. A combination of these shapes has resulted in a new antenna shape: the folded bow-tie antenna. An analysis of three candidates of this new antenna has been presented. In addition, the isolation problem of the feeding antenna from the water has been taken into account in the design, adding also an internal isolation to be able to isolate the battery and the electrical circuit from the water. Next, a full comparison has been done to choose the best shape to achieve the requirements of the application. After finding the best antenna, some variations of the water properties have been done in order to study the effect of them in the behavior of the antenna. Finally, a study of the transmission level and channel attenuation in water (pure and impure) is presented.

The main conclusions are:

- FEKO software is the most suitable software for the UWB antenna design for underwater communications, mainly due to the mesh simulation properties and also due to the computational environment properties flexibility.
- The circular loop antenna and the bow-tie shapes are good starting points for the design. The return loss of the combination of both shapes in water shows a promising behavior.
- Three candidates have been found as a good shapes.
- The second candidate is the best one without internal isolation.
- If an internal isolation is placed inside the antenna, the best candidate is the first one.

- The third candidate does not show a good behavior when an isolation of air and teflon is placed inside.
- The size of the antenna is an important factor to take into account. The bigger the size is, the better the return loss level in low frequencies is.
- The changes in the medium of propagation affect at the return loss level of the antenna. However, the typical values of the conductivity and the permittivity of water do not affect this parameter too much.
- The transmission level in pure water is 5dB lower than in air. However, if the conductivity increases, the channel attenuation increases too. Conductivities greater than σ=0.1S/m do not allow a good communication in devices with more than 50cm of separation.

Future work includes manufacturing the antenna for the Smart-PEAS project developed at CAS. Then rigorous measurements of the antenna in the laboratory would be necessary to compare the results obtained with the simulations done in this thesis. It will allow proving the viability of the antenna in the project.

Appendix

5.1 The effect of the air-to-water boundary

An important consideration of the propagation signal waves is the effect on water surface. Propagation losses and the refraction angle are such that an electromagnetic signal crosses the air-to-water boundary and appears to radiate from a patch of water directly above the transmitter. The large refraction angle produced by the high permittivity launches a signal almost parallel with the water surface.

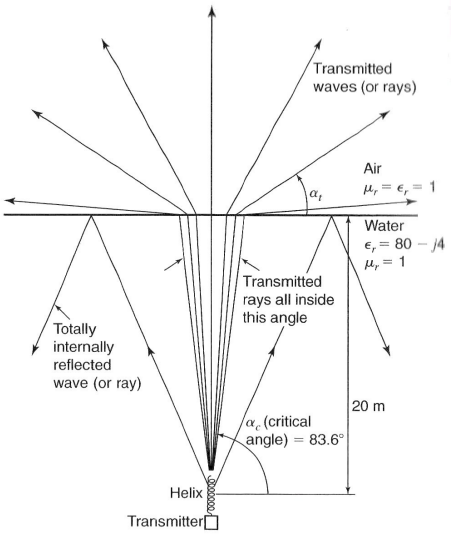

Figure 5.1: Example of the effect of the refraction of the air-to-water boundary

We can see an example in Figure 6.1. Rays from submerged antenna at angles α below $83,6°$ are totally internally reflected, while rays between $83,6°$ and $90°$ are transmitted through the surface into air above and spread out over almost $180°$[4].

The air path can be a crucial advantage for the electromagnetic waves between two antennas next to the surface. In comparison, acoustic signals cannot cross the water-to-air boundary, so the loss of the path between the two antennas through-water would be applied. A similar effect is seen at the seabed, where conductivity is much lower

than in the water.

The refraction loss due to the change in the medium can be defined on (6.1) [4]:

$$\gamma_{R_L} = -20 \log \{7.4586 \times 10^{-6} \times \sqrt{f/\sigma}\} \tag{5.1}$$

where γ_{R_L} is the refraction loss in dB.

This effect of the channel is important in the Smart-PEAS project because the path through the air may be better than for water, but the analysis of this effect is not our goal.

References

1. Marc Rhodes, "Underwater Electromagnetic Propagation", *http://www.hydro-international.com/issues/articles/ id697-Underwater_Electromagnetic _Propagation.html*

2. Alle-Jan van der Veen and Geert Leus, "Signal processing for communications", Delft University of Technology

3. Ahmed I. Al-Shammaa, Andrew Shaw, and Saher Saman, "Propagation of Electromagnetic Waves at MHz Frequencies Through Seawater", *IEEE Transactions on antennas and propagation*, Vol. 52, No. 11, November 2004

4. Lloyd Butler, "Underwater Radio Communication", *http://www.qsl.net/ vk5br /UwaterComms.htm*

5. Hansen, R C., "Radiation and Reception with Buried and Submerged Antennas", *IEEE Transactions on Antennas and Propagation*, May 1963.

6. "Linear and loop antennas", *www.ece.rutgers.edu/ orfanidi/ewa/ch16.pdf*

7. Daniel Andersson, "Design Challenges for UWB radar design", *radarbolaget*, 2008

8. Alexander Vorobyov, "Planar Elliptically Shaped Dipole Antenna Radio", pp. 1-7, 2008

9. "First Report and Order (FCC 02-48). Action by the Comission February 14, 2002. New Public Safety Applications and Broadband internet access among uses envisioned by FCC authorization of Ultra-Wideband Technology".

10. Balanis, "Antenna Theory, Analysis and Design".

11. *CST MICROWAVE STUDIO, Tutorials*, CST-Computer Simulation Technology, 2003.

12. K. Kurokawa, "Power waves and the scattering matrix", *Microwave Theory and Techniques, IEEE Transactions on*, vol. 13, no. 2, pp. 194-202, Mar 1965.

13. "IEEE standard definitions of the terms for antennas", *IEEE Transactions on Antennas and Propagations*, vol. AP-31, no. 6, 1983.

14. M. Pausini, "Autocorrelation Receivers for Ultra Wideband Wireless Communications", pp 10-12, 2007.

15. "Kaye & Laby, Tables of Physical and Chemical Constants, National Physical Laboratory, *http://www.kayelaby.npl.co.uk/*

16. Vyacheslav V. Komarov and Juming Tang, "Dielectric Permittivity and loss factor of tap water at 915MHz", *MICROWAVE AND OPTICAL TECHNOLOGY LETTERS* Vol. 42, No. 5, September 2004

17. Schlumberger Excellence in Educational Development, "Conductivity of water", *http://www.seed.slb.com*

18. Martin Chaplin, "Water structure and science", *http://www.lsbu.ac.uk/water/microwave.html*